



**UCLouvain**

Institute of Mechanics,  
Materials and Civil Engineering

## Robust optimisation of the pathway towards a sustainable whole-energy system

A hierarchical multi-objective  
reinforcement-learning based approach

Doctoral dissertation presented by

**Xavier RIXHON**

in partial fulfillment of the requirements for  
the degree of Doctor in Engineering Sciences

December 2023

### Thesis committee

Pr. Francesco CONTINO (supervisor, UCLouvain)

Pr. Hervé JEANMART (supervisor, UCLouvain)

Dr. Stefano MORET (ETH Zurich)

Pr. Sylvain QUOILIN (ULiège)

---

---

© 2023  
Xavier Rixhon  
All Rights Reserved

---

---

---

# Contents

<b>Symbols</b>	<b>iii</b>
<b>1 The atom-molecules dilemma: deterministic and uncertainty analyses</b>	<b>1</b>
1.1 Deterministic impact of integrating small modular reactor (SMR) in 2040 . . . . .	2
1.1.1 Power sector . . . . .	3
1.1.2 System-level impacts . . . . .	3
1.1.3 Non-power sectors . . . . .	5
1.2 Uncertainty quantification on the cost, the atom and the molecules . . . . .	8
1.2.1 Total transition cost . . . . .	9
1.2.2 Atom and molecules . . . . .	11
1.2.3 Local renewables . . . . .	16
<b>Bibliography</b>	<b>19</b>
<b>A EnergyScope Pathway: Its choice and its formulation</b>	<b>29</b>
A.1 EnergyScope Pathway: The right model to choose . . . . .	29
A.2 EnergyScope Pathway and its linear formulation . . . . .	35
A.2.1 The starting point: a scenario analysis model . . . . .	35
A.2.2 Extending the model for pathway optimisation . . . . .	39
<b>B Case study: the Belgian energy system</b>	<b>47</b>
B.1 Belgian energy system in 2020 . . . . .	47
B.2 Belgian energy transition pathway towards carbon-neutrality in 2050 . . . . .	47
B.2.1 Greenhouse gases and primary energy . . . . .	49
B.2.2 Electricity sector: Capacities and yearly balance . . . . .	51
B.2.3 Costs: Investments and operation . . . . .	53
B.3 Myopic versus perfect foresight pathway optimisation . . . . .	57

B.4	Assessment of different emissions-trajectories . . . . .	59
B.4.1	CO <sub>2</sub> -budget versus linear decrease of emissions . . . . .	61
B.4.2	Comparison without restriction on greenhouse gases (GHG) .	61
B.5	Uncertainty characterisation for the 5-year steps transition . . . . .	63
<b>C</b>	<b>Pathway optimisation under uncertainties</b>	<b>67</b>
C.1	Total transition cost . . . . .	67
C.2	Imported renewable electrofuels . . . . .	70

---

---

# Symbols

## Acronyms

<b>API</b>	application programming interface
<b>BECCS</b>	bioenergy with carbon capture and storage
<b>BEV</b>	battery electric vehicle
<b>BTX</b>	benzene, toluene and xylene
<b>CAPEX</b>	capital expenditure
<b>CCGT</b>	combined cycle gas turbine
<b>CCS</b>	carbon capture and storage
<b>CHP</b>	combined heat and power
<b>CNG</b>	compressed natural gas
<b>DHN</b>	district heating network
<b>ESOMs</b>	energy system optimisation models
<b>EnergyScope TD</b>	EnergyScope Typical Days
<b>EUD</b>	end-use demand
<b>FC</b>	fuel cell
<b>GDP</b>	gross domestic product
<b>GHG</b>	greenhouse gases
<b>GSA</b>	global sensitivity analysis
<b>GWP</b>	global warming potential
<b>HP</b>	heat pump
<b>HT</b>	high-temperature
<b>HVC</b>	high value chemicals
<b>ICE</b>	internal combustion engine
<b>IEA</b>	International Energy Agency
<b>IPCC</b>	intergovernmental panel for climate change
<b>IQR</b>	interquatile range

<b>LCA</b>	life cycle assessment
<b>LCOE</b>	levelised cost of energy
<b>LFO</b>	light fuel oil
<b>LOO</b>	leave-one-out
<b>LPG</b>	liquefied petroleum gas
<b>LT</b>	low-temperature
<b>MDP</b>	Markov decision process
<b>MMSA</b>	Methanol Market Services Asia
<b>MTBE</b>	methyl tert-butyl ether
<b>MTO</b>	methanol-to-olefins
<b>NED</b>	non-energy demand
<b>NG</b>	fossil gas
<b>NN</b>	neural network
<b>NRE</b>	non-renewable energy
<b>NSC</b>	naphtha steam cracker
<b>OPEX</b>	operational expenditure
<b>PC</b>	principal component
<b>PCA</b>	Principal Component Analysis
<b>PCE</b>	Polynomial Chaos Expansion
<b>PDF</b>	probability density function
<b>PV</b>	photovoltaic
<b>RE</b>	renewable energy
<b>RL</b>	reinforcement learning
<b>SAC</b>	Soft Actor Critic
<b>SDGs</b>	Sustainable Development Goals
<b>SMR</b>	small modular reactor
<b>SVD</b>	singular value decomposition
<b>UQ</b>	Uncertainty Quantification
<b>VRES</b>	variable renewable energy sources

---

---

## List of publications

Limpens, G., **Rixhon, X.**, Contino, F., & Jeanmart, H. (2024). “*EnergyScope Pathway: An open-source model to optimise the energy transition pathways of a regional whole-energy system.*” In Applied Energy, (Vol. 358). URL: <https://doi.org/10.1016/j.apenergy.2023.122501>

**Rixhon, X.**, Limpens, G., Coppitters, D., Jeanmart, H.,& Contino, F.(2022). “*The role of electrofuels under uncertainties for the Belgian energy transition.*” In Energies (Vol. 14). URL: <https://doi.org/10.3390/en14134027>

**Rixhon, X.**, Tonelli, D., Colla, M., Verleysen, K., Limpens, G., Jeanmart, H. ,& Contino, F.(2022). “*Integration of non-energy among the end-use demands of bottom-up whole-energy system models.*” In Frontiers in Energy Research, Sec. Process and Energy Systems Engineering, (Vol. 10). URL: <https://doi.org/10.3389/fenrg.2022.904777>

**Rixhon, X.**, Colla, M., Tonelli, D., Verleysen, K., Limpens, G., Jeanmart, H., & Contino, F.(2021). “*Comprehensive integration of the non-energy demand within a whole-energy system: Towards a defossilisation of the chemical industry in Belgium.*” In proceedings of ECOS 2021 conference (Vol. 34, p. 154).

**Rixhon, X.**, Limpens, G., Contino, F., & Jeanmart, H. (2021). “*Taxonomy of the fuels in a whole-energy system.*” In Frontiers in Energy Research, Sec. Sustainable Energy Systems, (Vol. 9). URL: <https://doi.org/10.3389/fenrg.2021.660073>

Limpens, G., Coppitters, D., **Rixhon, X.**, Contino, F., & Jeanmart, H. (2020). “*The impact of uncertainties on the Belgian energy system: application of the Polynomial Chaos Expansion to the EnergyScope model.*” In proceedings of ECOS 2020 conference (Vol. 33, p. 711).

---

---

## **Chapter 1**

# **The atom-molecules dilemma: deterministic and uncertainty analyses**

On top of scenarios with more profound behavioural changes, variety of technological pathways are often investigated to meet the ambitions of climate change mitigation. For instance, in their work, Climact and VITO [1] assessed different scenarios for a climate neutral Belgium by 2050. Depending on the scenarios, the emphasis is put on a higher electrification of the whole-energy system, a higher consumption of hydrogen or more complex molecules (i.e. electrofuels) or a bigger reliance on biomass and the related bioenergy with carbon capture and storage (BECCS). Besides these, “unicorn” technologies are also investigated [2]. These are technological solutions that have not (yet) reached a high enough maturity, i.e. TRL 3 to 7, or facing non-techno-economic hurdles (i.e. social acceptance) to be currently deployed on a large scale. Among others, nuclear energy, potentially in the form of small modular reactor (SMR), finds an interest in the literature [3, 4] as well as in actual current investments, in Belgium for instance [5].

In a society with an increasing electricity demand, notably due to the electrification of sectors like mobility, low-temperature heat or industry, and a deeper integration of variable renewable energy sources (VRES), there seems to be a case for nuclear energy to produce a reliable low-CO<sub>2</sub>emission electricity [6], especially given the willingness to phase out of imported Russian fossil fuels anchored in the European REPowerEU Plan [7]. Unlike fossil natural gas that is a “flow-based” resource, uranium is “stock-based”, which favours the security of electricity supply, in case of a conflict like the invasion of Ukraine, for instance.

As pointed out by IAEA [6]: “Country specific energy studies are needed as a prerequisite to the decision of following the nuclear route.”

Even though in a country like Belgium, reaching the goal of energy transition will not be a “winner-takes-all” situation but rather a combination of solutions, implemented simultaneously [8], this chapter focuses on this atom-molecules dilemma in two ways. First, Section 1.1 targets the impact of integrating SMR from 2040 onward on the whole-energy system, in a deterministic way (i.e. considering only nominal values of the parameters). Second, accounting for uncertainties as presented in section ??, section 1.2 will identify the key factors driving higher or lower imports of electrofuels as well as the installation of SMR.

**Disclaimer:** Relying on “local” nuclear energy for some (or on importing electrofuels from abroad for others) is highly controversial. On top of purely techno-economic aspects, non-exhaustively mentioned beforehand, there are other ethical, societal or even political considerations to account for when addressing this question. Like the rest of this thesis, the purpose here is only to expose the impact of integrating SMR in the Belgian energy landscape, on a strictly techno-economical point of view. This is why, for the sake of transparency, the model and the data are documented and openly available online [9] and in the Appendices A and B.

## Contributions

- Pathway UQ
- Contrast analysis between atom and molecules and local renewables
- Influence of the parameters on the import of molecules and the installation of SMR
- Often compared, if not opposed, to local renewables like wind and solar [10, 11], this chapter rather assesses the integration of nuclear energy in the future versus the need to import renewable molecules from abroad.

### 1.1 Deterministic impact of integrating SMR in 2040

In this section, like in the rest of the thesis, the **REF** case is without any deployment of SMR anytime during the transition and whereas in the **SMR** case this technology is available, up to 6 GW, from 2040 onward. After investigating the deployment of SMR through the power sector, the first part of this section focuses on this impact on

macro/system-level considerations (i.e. overall transition costs, primary energy mix and yearly emissions per sector). The second part will address the impact of SMR on each of the other sectors of the system.

### 1.1.1 Power sector

Figure 1.1 shows that SMR is deployed as soon as available, i.e. 2040, to their maximum capacity, i.e. 6 GW, substituting other flexible power generation units: no ammonia-combined cycle gas turbine (CCGT) at the end of the transition and the anticipatory reduction of methane CCGT (i.e. 2.1 GW in 2040 versus 3.7 GW for the REF case). To a lesser extent, the last 2% deployment of solar-photovoltaic (PV) is slightly delayed as the capacity in 2025 is 1.3 GW smaller than in the REF case. Overall, given the smaller efficiency of SMR, i.e. 40% versus 51% for ammonia-CCGT, the restriction on yearly availability and the slightly higher electrification (Figure 1.2), the total power capacity installed by 2050 is 3.5% higher for the SMR case.

**Compare here with EnergyVille - PATHS2050.**

When assessing the electricity production-versus-consumption-balance (Figure 1.2), SMR, as a cheaper, flexible and low-emitting power generation system, produces to its full capacity, given the 15% maintenance off-time assumed in this work: 44.6 TWh. By 2050, it represents 24.6% of the total electricity production which is less than the current share of conventional nuclear in Belgium, 38.5%. This resurgence of nuclear electricity occurs at the expense of other, although more efficient technologies: CCGT and industrial combined heat and power (CHP). Besides the unchanged end-use-demand, we observe a slight increase of the electrification of the rest of the system: +9.4% which corresponds to +5.8 TWh, mostly consumed by electric heaters in industry (+48%) to produce industrial high-temperature heat.

### 1.1.2 System-level impacts

First of all, as far as the objective function (i.e. the total transition cost) is concerned, Figure 1.3 shows that the 6 GW SMR installed from 2040 allow reaching a 3.3% (-36.9 b€, ~6% of the Belgian GDP) cheaper overall transition. Interestingly, as the model can freely spend the constrained CO<sub>2</sub>-budget over the transition, knowing ahead (i.e. perfect foresight) that cheaper and low-emitting SMR will be available in the future, cost-savings, that are more important after 2040, also occur before 2040. This is mostly due to the extended use of cheaper light fuel oil (LFO) at the beginning of

#### 4 Chapter 1. The atom-molecules dilemma: deterministic and uncertainty analyses

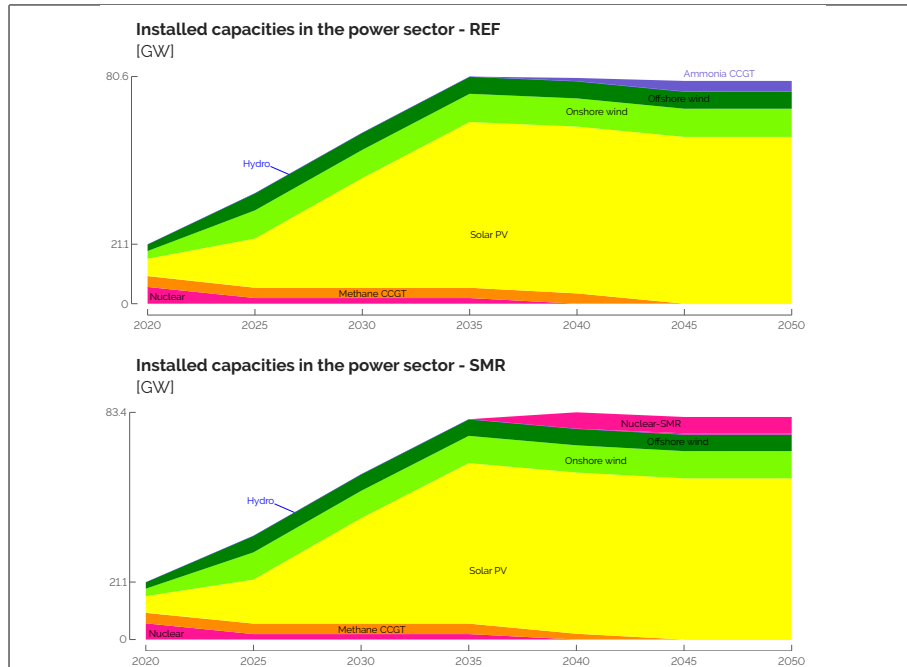
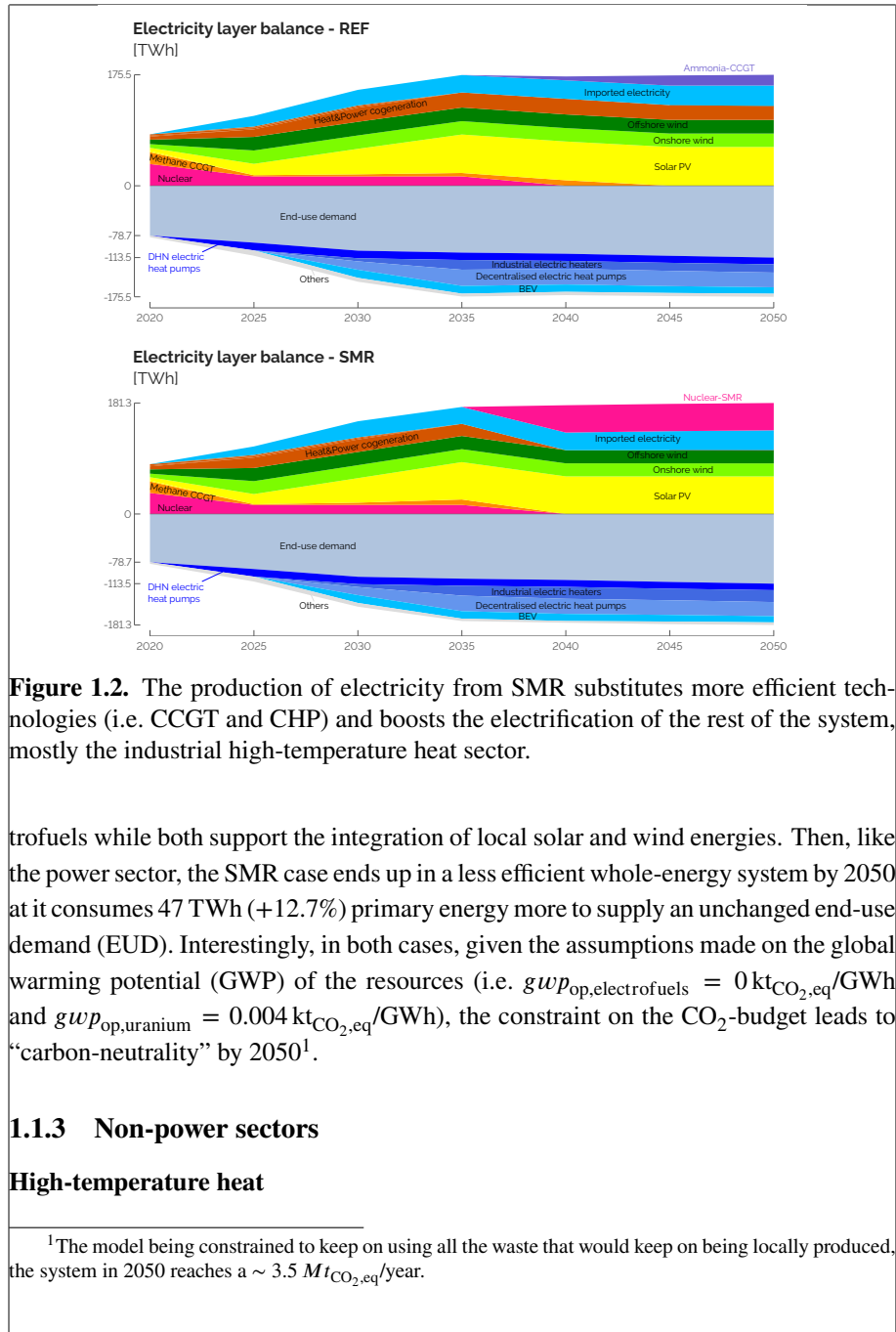


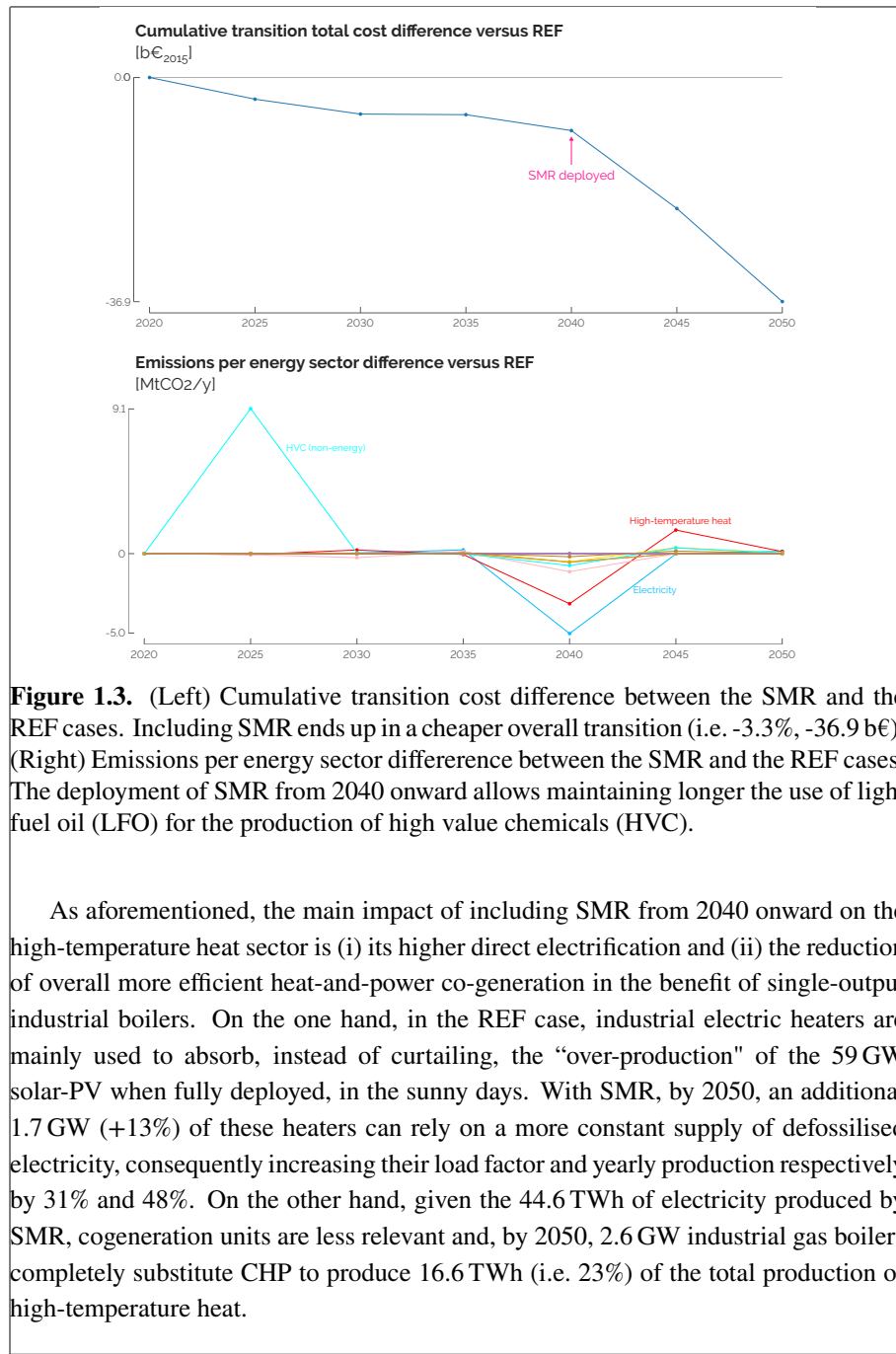
**Figure 1.1.** As soon as available (i.e. 2040), small modular reactor (SMR) is deployed to their maximum potential (i.e. 6 GW) to substitute more expensive flexible generation units (i.e. gas and ammonia CCGT).

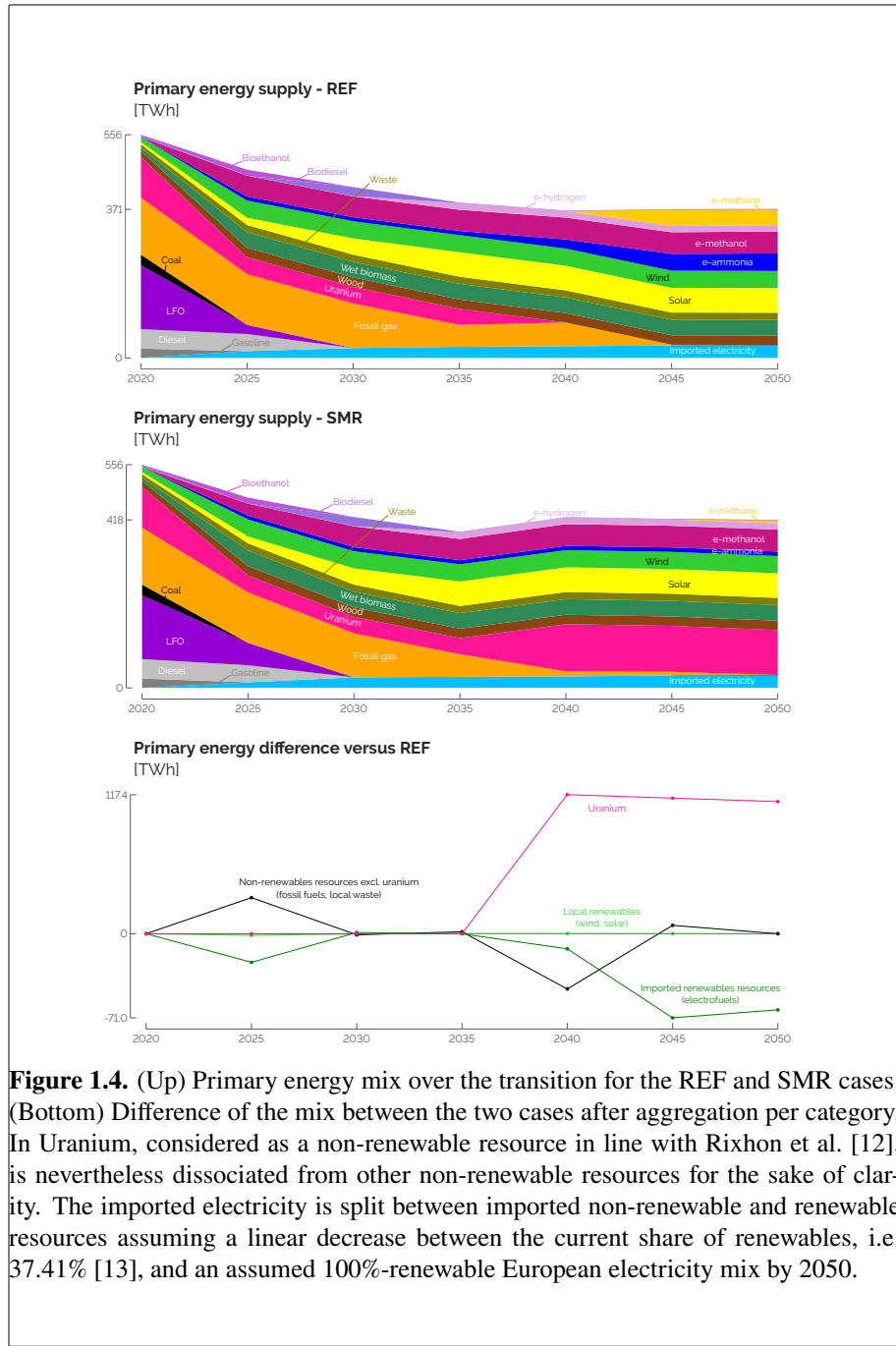
the transition to produce high value chemicals (HVC), that is then compensated by the deployment of SMR (Figure 1.3). Then, the capital-intensive investments in SMR, mostly recovered by the end of the transition as salvage value, are widely compensated by the smaller resource-related OPEX. This leads, at the end, aggregating the OPEX and the annualised CAPEX, to a system that is yearly 8.8% less expensive by 2050.

Then, considering the primary energy mix shown in Figure 1.4, three phases in the transition can be identified. Before 2040, thanks to the perfect foresight approach, the model finds it more economical in 2025 to keep on using 33.2 TWh of LFO to produce HVC through naphtha/LPG-cracking. In 2040, uranium-driven SMR substitutes the electricity originally produced from industrial CHP and CCGT running respectively on fossil gas and renewable ammonia. Finally, from 2045 onward, the significant drop in the consumption of electrofuels comes from the same industrial CHP. This is the illustration of the atom-molecules dilemma where the consumption of local renewables is, on its side, not much affected. In other words, SMR competes with importing elec-



## 6 Chapter 1. The atom-molecules dilemma: deterministic and uncertainty analyses





### **Low-temperature heat**

This sector is marginally impacted. In both cases, the major shift of supply from decentralised to centralised productions operates early in the transition, to hit the constraint that district heating network (DHN) cannot supply more than 37% of the low-temperature (LT)-heat production. Then, from a mix between oil (53%), gas (43%) and wood (4%) boilers for the decentralised production of LT-heat in 2020, the system progressively shifts towards electric heat pump (HP) only. Similarly for the centralised production of LT-heat, electric HP remains the most efficient and economic option.

### **Mobility**

The passenger mobility is not affected either as the electrification of the system is preferentially done in this sector with battery electric vehicle (BEV) progressively substituting internal combustion engine (ICE) cars for the private sector. About the public mobility, trains and tramways supply their *a priori* set maximum share, respectively, 50% and 30% complemented by compressed natural gas (CNG) buses substituting diesel-driven buses. Similarly, considering the freight transport, technology shifts (i.e. from diesel to fuel cell (FC) trucks) or modal shares (i.e. 53%-47% split between fossil gas (NG) and (bio)-diesel boats) are identical between the two cases.

### **Non-energy demand**

The supply of ammonia (i.e. from Haber-Bosch to direct import of renewable ammonia) and methanol (i.e. import of renewable methanol) are unchanged between the two cases. However, as introduced previously, to produce HVC, the full substitution of naphtha/LPG-cracking by methanol-to-olefins (MTO) is delayed as the emissions of the former are compensated by the later integration of SMR.

## **1.2 Uncertainty quantification on the cost, the atom and the molecules**

*“It is difficult to make predictions, especially about the future.”* (Niels Bohr, foundational contributor to the understanding of atomic structure and quantum theory). Besides the deep understanding of the deterministic results, it is important to challenge these conclusions out-of-sample, accounting for the uncertainty of the parameters. To mitigate the computational burden, we have used the Polynomial Chaos Expansion (PCE) approach (Section ??) on the monthly version of EnergyScope Pathway. As de-

tailed by Limpens et al. [14], this simplified model does not implement daily storage technologies and integrates much more easily intermittent renewables (PVs and wind turbines) in the system as the daily supply-demand intermittency and mismatch are not at stake. Consequently, it requires less flexibility options (i.e. electrification of the heating sector or import of electricity from the neighbouring countries) and ends up with a cheaper transition (-3%). Although, it allows to quantify the full set of 34 uncertain parameters (i.e. 1260 samples for an order-2 PCE), and avoid the computational burden of the hourly pathway. Nevertheless, comparing the Uncertainty Quantification (UQ) on the hourly pathway with a limited set of uncertain parameters and on the monthly model, Appendix C.1 shows that the most impacting parameters are correctly captured by the latter.

After briefly assessing the global sensitivity analysis (GSA) on the objective function of the model, the total transition cost, this section investigates more deeply the atom-molecules dilemma. This time, the Sobol' indices are computed for import of renewable molecules and installed capacities of SMR.

### 1.2.1 Total transition cost

Exhaustively listed in Appendix C.1, Table 1.1 gathers the most impacting parameters<sup>2</sup> on the total transition cost, highlighting the cost of purchasing electrofuels as well as the potentiality to install SMR and its CAPEX. The former is the most impacting parameter whereas the two others have much lower influence on the variation of the total transition cost. Given the uncertainty characterisation presented in Section ??, there are 60% chance that no SMR could be installed. In other words, the variation of the parameter  $f_{\max, \text{SMR}}$  has zero impact on the variation of the total transition cost in 60% of the samples. Then, in perspective with the local sensitivity analysis of Section 1.1, the 3.3% reduction has been observed when SMR is installed from 2040 onward. This represents only 10% of the samples. Moreover, given its characteristics detailed in ??, mostly its cheap and low-emitting fuel (i.e. uranium) and the long lifetime leading to lower annualised CAPEX and higher salvage value, this explains why SMR has this lower impact. On the contrary, more expensive renewable electrofuels are always imported, to a smaller or larger extent depending on the sample. For instance, in the REF case (Section 1.1.2), the imported electrofuels represent, by 2050, 152.9 TWh (i.e. 41% of the primary energy mix) with an average 93€/MWh cost of purchasing and, over the entire transition, a 273 b€ cumulative OPEX (i.e. 25% of the total transition cost).

<sup>2</sup>Per Turati et al. [15], parameters are considered as “impacting” if their Sobol’ index is above the threshold =  $1/d$ ,  $d$  being the total number of uncertain parameters after the pre-selection phase. In this case,  $d = 34$ , and, consequently, the threshold is equal to 2.9%.

**Table 1.1.** Total Sobol' indices of the uncertain parameters over the total transition cost. Where the cost of purchasing electrofuels is the top-1 parameter, SMR-related parameters have a negligible impact on this cost.

Parameter	Ranking	Sobol' index
<b>Purchase electrofuels</b>	1	47.4%
Industry EUD	2	23.5%
Interest rate	3	11.0%
Purchase fossil fuels	4	6.9%
:	:	:
<b>Potential capacity SMR</b>	11	0.9%
:	:	:
<b>CAPEX SMR</b>	32	<0.1%

Given the relatively wide uncertainty range (i.e. up to [-30.8%; +24.0%] by 2050) and, above all, the major share among the total demand, between 53% and 60%, the industrial EUD is the second most impacting parameter. Then, as the driving factor for the annualisation and the salvage value of the assets, the interest rate has a 11% Sobol' index<sup>3</sup>. Finally, similarly to electrofuels, the cost of purchasing fossil fuels is also to consider in the perspective to reduce the uncertainty over the total transition cost. However, due to the ambitious CO<sub>2</sub>-budget, phasing out of fossil fuels is urgent and makes their uncertain impact smaller than their renewable alternatives.

Figure 1.5 shows the probability density function (PDF) of the total transition cost given the 1260 samples. Stretching between 680 b€ and 1940 b€, the mean, the median and the nominal value (i.e. REF case) are close to each other, respectively 1160 b€, 1150 b€ and 1080 b€. Similarly to the analysis carried out by Coppitters and Contino [17], one observes here that the distribution is right-skewed. It could then be qualified as "fragile" as the top 50% of the samples cover a bigger range (i.e. between 1150 and 1940) than the bottom 50% of the samples (i.e. between 680 and 1150). In other words, the bad scenarios, resulting in a total transition cost higher than the median, have a bigger effect on this cost.

<sup>3</sup>It is important to note here that the model considers an overall interest rate for the entire system (i.e. 1.5% as a nominal value). In practice, the interest rate would vary depending on the technology investment risk. This variation would have, for instance, a major impact on the levelised cost of energy (LCOE) of technologies like nuclear power plants [16], given the important capital needs and long time horizons [3].

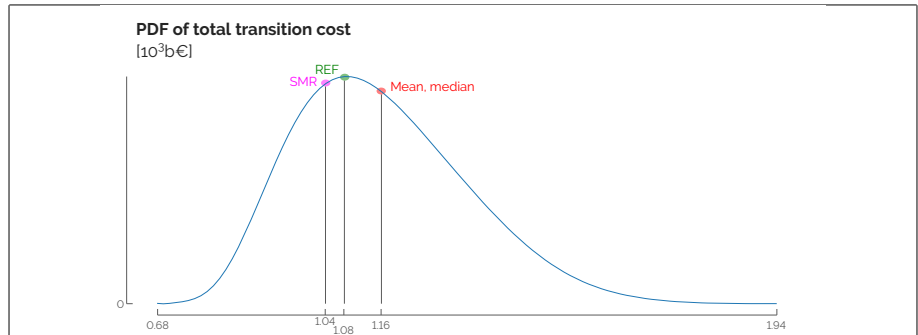


**Figure 1.5.** probability density function (PDF) of the total transition cost. The mean,  $\mu = 1.16 \cdot 10^3$  b€, is slightly higher than the median ( $P_{50} = 1.15 \cdot 10^3$  b€) and the nominal cases cost,  $1.08 \cdot 10^3$  b€ and  $1.04 \cdot 10^3$  b€ respectively for the REF and SMR cases. Also, with a standard deviation,  $\sigma = 185$  b€, a 95%-confidence interval would be about  $[0.8; 1.5] \cdot 10^3$  b€.

### 1.2.2 Atom and molecules

The samples used to carry out the GSA on the total transition cost, also provide the distribution of other outputs of the model. Among them, Figure 1.6 shows the evolution of the import of renewable electrofuels over the transition.

As the general trends are increasing, discrepancies exist between the different energy carriers. E-methane, as the renewable alternative to fossil natural gas, substitutes it, sometimes at a very early stage of the transition, 2025, and to a somehow unrealistically large extent, 173 TWh, which is more than 13% more than the total import of electrofuels in the REF case. The necessity to import this molecule is progressive through the transition to supply mostly industrial CHP and boilers.

E-hydrogen becomes rapidly the main stream of hydrogen in the system, on top of steam-methane-reforming or electrolysis, to reach a median and a maximum values of, respectively 13.6 TWh and 40.7 TWh in 2050. Hydrogen is more frequently used in the mobility sector. Like in the REF case, fuel cell trucks are often the first option but, in some outlying cases, fuel cell cars and buses appear to completely substitute respectively BEV cars and CNG buses by 2050. Moreover, some samples lead to local production of methanol via the methanolation process, to produce up to 16.3 TWh of methanol (i.e. 30% of the total supply of methanol of the nominal REF and SMR cases).

Then, the imported e-ammonia, becoming rapidly cost-competitive against its fossil alternative (??), quickly substitutes it and the Haber-Bosch process. Where the initial purpose of ammonia is to satisfy a relatively limited non-energy demand (NED)

## 12 Chapter 1. The atom-molecules dilemma: deterministic and uncertainty analyses

(i.e.  $10 \pm 3$  TWh by 2050), the variation of its import is mostly due to the higher or lower need for ammonia-CCGT as a flexible option to produce electricity. From 2035, out of the four considered electrofuels, the imported e-ammonia is the one exhibiting the largest uncertainty with, for instance, an interquartile range (IQR)<sup>4</sup> of about 50 TWh. In some extreme cases, e-ammonia is the most imported molecules, i.e. up to 233 TWh or 63% of the total primary mix in the REF case in 2050.

Likewise, e-methanol early becomes the selected option to supply methanol even though alternatives like biomass-to-methanol or synthetic methanolation exist in some outlying cases. Given its lower non-energy demand (NED) (i.e.  $1.5 \pm 0.5$  TWh<sub>NED, methanol</sub> by 2050), the variation of imported e-methanol is almost exclusively due to its role in the industrial production of HVC, i.e. 78% of the total NED, through the methanol-to-olefins (MTO) process. In some rare samples, methanol is also used to supply the freight transport sector via boats or trucks.

Appendix C.2 gives a more detailed information. On the one hand, it compares the statistics (i.e. quartiles and median) with the quantity of imported electrofuels in the REF and SMR cases. On the other hand, this appendix shows the distributions of the different sources of supply and consumption of gas, hydrogen, ammonia and methanol.

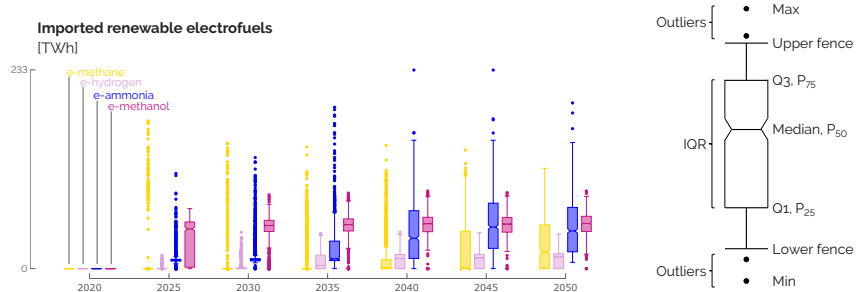


**Figure 1.6.** Distribution of the imported renewable electrofuels over the transition. Starting from no electrofuel in 2020, their respective import rises progressively along the transition (i.e. increasing median) at different growth rates and with different ranges of values. Observations being either 1.5 times the interquartile range (IQR) less than the first quartile (Q1) or 1.5 times the interquartile range greater than the third quartile (Q3) are defined as outliers.

After investigating the distribution of imports of electrofuels over the transition, this part assesses the space of uncertainties, like Pickering et al. [18] who investigated the space of feasibility to reach carbon neutrality in Europe. Figures 1.7 and 1.8 give

<sup>4</sup>The interquartile range is the difference between the third quartile ( $Q3$  or  $P_{75}$ ) and the first ( $Q1$  or  $P_{25}$ ). It is an indicator of statistical dispersion around the median,  $Q2$  or  $P_{50}$ .

the trend lines of the key parameters for these imports in 2050<sup>5</sup>, as well the installed capacities of SMR. Next to the name of a parameter, one can read its Sobol' index versus the output of interest<sup>6</sup>. Box plots also point out the distribution of this output for the extreme low or high values of some parameters.

As aforementioned, the industrial EUD impacts the most the import of e-methane. This parameter directly dictates the demand of industrial high-temperature heat for which industrial gas CHP, and industrial gas boilers to a lower extent, represent, on average over all the samples, respectively 25.6% and 6.1% of the total production. Then, considering the smaller-impact parameters, we notice that SMR plays a non-negligible role. Indeed, if deployed, SMR produces abundant low-emitting electricity for industrial electric heaters that substitute, even completely in some cases, gas alternatives. This confirms the observation made in Section 1.1.3. Highly available local biomass also leads to smaller import of e-methane to supply bio-hydrolysis and produce methane-equivalent gas. Finally, and surprisingly, costs of purchasing electrofuels and fossil fuels have a positive and negative correlation with the amount of e-methane, respectively. In other words, by 2050, more expensive electrofuels induce to more e-methane import and *vice versa* for the fossil fuels. Given the techno-economic optimum sought by EnergyScope, if electrofuels are more expensive, the system will, overall, import less of them, especially e-ammonia, mainly used by CCGT. Subject to the CO<sub>2</sub>-budget for the transition, the system goes towards more efficient technologies, like industrial methane-CHP to substitute e-ammonia-CCGT in the production of electricity. First running on fossil natural gas, these CHP consume more e-methane by 2050. In the contrary, if electrofuels are cheaper, there is more import of them, and especially of e-ammonia. This leaves room for more emitting and cheaper resources to be used while respecting the CO<sub>2</sub>-budget, i.e. coal in industrial boilers that produce, in these cases, on average 24% of the high-temperature (HT) heat in 2050. Consequently, there is smaller investment in methane CHP, and consequently import of e-methane as more abundant renewable electricity is produced via e-ammonia-CCGT and more HT-heat is supplied by industrial coal boilers. Even though we might expect that no more coal will be consumed in Belgium by 2050, the model still has the opportunity to use it if the CO<sub>2</sub>-budget allows it. About the cost of purchasing fossil fuels, the parameter has mainly an impact on the import of fossil NG as the most versatile energy carrier in the whole-energy system. If NG is more expensive, the system will import less of

<sup>5</sup>The authors picked this specific year as it is the one where electrofuels, if imported, are imported in the largest amount, in general, compared to the other years of the transition.

<sup>6</sup>For these outputs of interest, different from the total transition cost, the leave-one-out (LOO) error is generally higher than the threshold of 1 % defined in Section ???. Consequently, the Sobol' indices are less accurate but already allow a fair relative comparison between the different parameters.

it. Subsequently, the investments in methane-CHP and boilers are more limited. This ends up in smaller need for e-methane by 2050.

In relation to e-hydrogen, the sensitivity analysis highlights its dependence on various driving parameters, particularly those linked to the transport sector. As depicted in Figure C.1 in Appendix C.2, the utilisation of e-hydrogen is most prevalent in FC trucks, followed by FC cars and buses to a lesser extent. The adoption of fuel cell engines in trucks contributes, on average, to 63.5% of the total road freight transport, thereby affecting the level of e-hydrogen imports. Consequently, the smaller is the CAPEX of fuel cell engines, the more the system imports e-hydrogen. Similarly, the cost of purchasing electrofuels influences e-hydrogen imports. Subsequently, the cost of purchasing biofuels emerges as the third most influential parameter. Indeed, biodiesel trucks are the mostly picked alternative to FC trucks to provide, on average, 27.6% of the total. Additionally, CNG buses are preferred in public road transport (34.9%), followed by FC buses (11.2%) competing with biodiesel and hybrid biodiesel buses, accounting for 27.8% and 26.1%, respectively. Finally, the last noticeable parameter at stake is the CAPEX of electric vehicles. In competition with BEV that stand for 83.4% on average of the private mobility sector, the cheaper these cars are, the more cost-competitive are these vehicles, and vice versa, versus FC cars (i.e. 13.7% of the total passenger mobility, on average).

As already pointed out in Section 1.1.1, the installation of SMR drastically reduces the import of e-ammonia. As ammonia CCGT is the biggest consumer of ammonia by the end of the transition, low-emitting and cheap electricity flexibly produced by SMR substitutes the CCGT. With a higher cost of purchasing electrofuels, this import of e-ammonia drops down to 7.3 TWh, 83.4% less than in the REF case. Then, with a 9%-Sobol' index, industrial EUD also influences the need for this molecule, due to its NED.

The conclusions are more straightforward for the import of e-methanol and the installed capacity of SMR. For the former, industrial EUD is, by far (i.e. 81% Sobol' index), the key factor. Due to its own NED but, above all, since it is the low-emitting alternative picked by the model to supply the significant NED of HVC, the lower this demand, the lower the need to import e-methanol, and vice versa. For the latter, it is the availability of the technology that drives its installation. Not shown here but all the samples of the GSA highlight that SMR is installed to its maximum capacity, i.e. 6 GW, as soon as possible. In other words, the only parameter "Potential capacity

SMR” dictates the installation of this technology<sup>7</sup>. Surprisingly, the [-40%; +44%] variation of its CAPEX has a negligible impact, with a Sobol’ index of 0.9%.

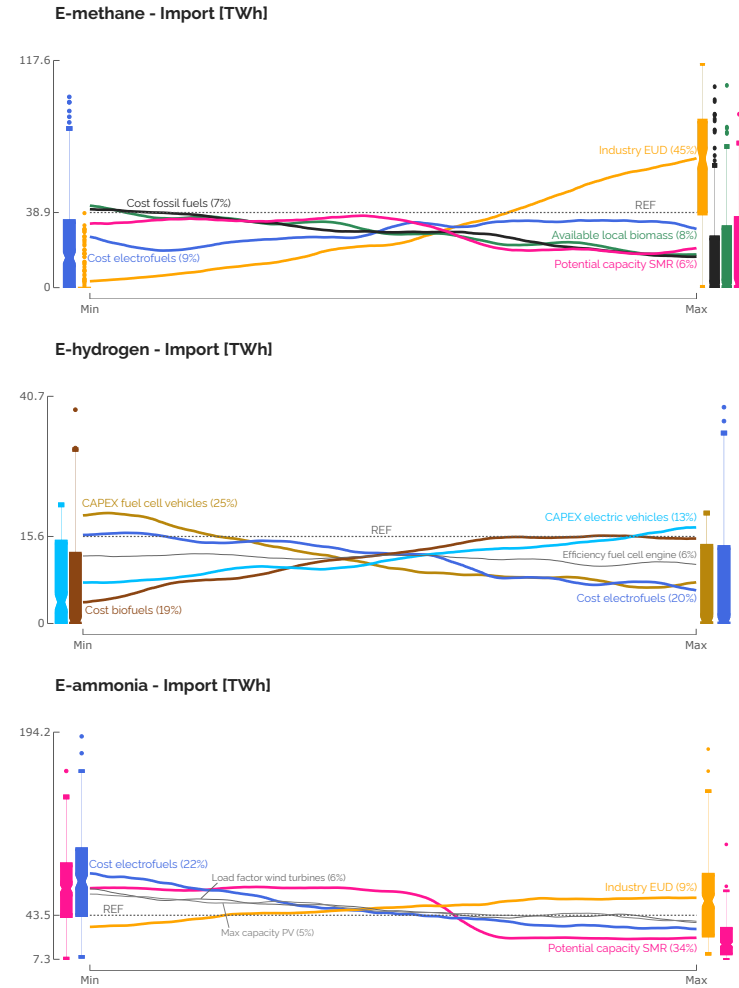


**Figure 1.7.** Trend lines of the key parameters on the import of e-methane, e-hydrogen and e-ammonia. Around these lines, box plots point out the distribution of the output of interest for the extreme values (either bottom-15% or top-15%) of some parameters. The grey dashed line gives the value of the output of interest in the REF case. Part A

<sup>7</sup>In practice, we observe that as soon as this parameter is equal or higher than 0.9, 0.8 and 0.6, 6 GW SMR is installed from 2040, 2045 and 2050, respectively.

## 16 Chapter 1. The atom-molecules dilemma: deterministic and uncertainty analyses

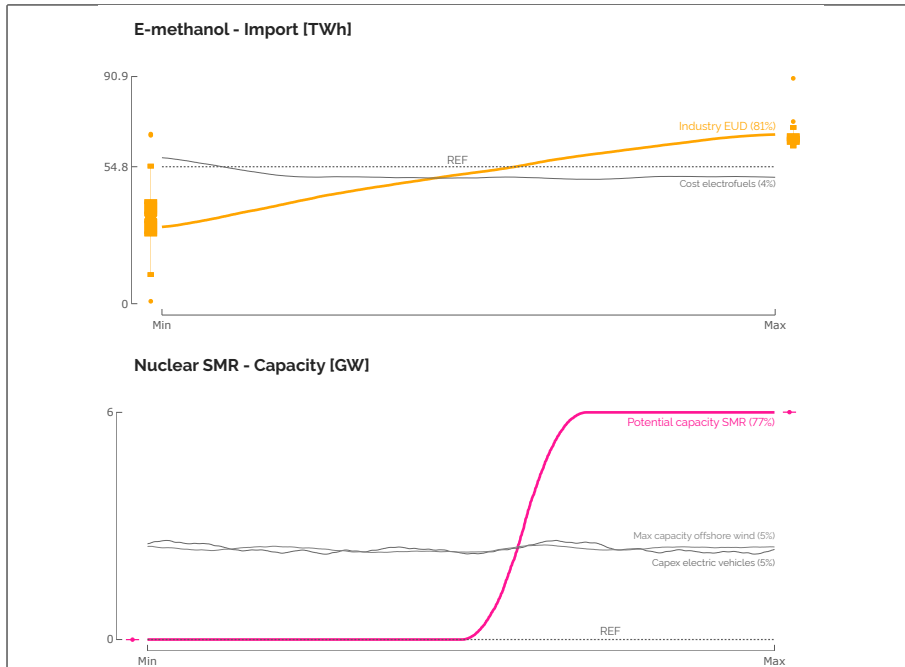


**Figure 1.8.** Trend lines of the key parameters on the import of e-methanol and the installed capacity of SMR, in 2050. Around these lines, box plots point out the distribution of the output of interest for the extreme values (either bottom-15% or top-15%) of some parameters. The grey dashed line gives the value of the output of interest in the REF case. Part B

### 1.2.3 Local renewables

In line with results given in Section 1.1, the GSA shows that SMR has negligible impact on the deployment of local VRES (i.e. PV, onshore and offshore wind turbines). Figure 1.9 gives the evolution of Sobol' indices for the most impacting parameters on the deployment of PV and offshore wind<sup>8</sup>. The key factor that drives the installed capacities of these two technologies is mostly their respective maximum potential, especially at the end of the transition, much more than their CAPEX. Given its higher LCOE (?), PV is more impacted in the short-term by the variation on the cost of purchasing electrofuels supplying e-methane (and e-ammonia to a lesser extent) CCGT. However, this impact gets negligible by 2050.

<sup>8</sup> As the installed capacities of onshore wind is totally driven by the uncertainty on its maximum potential,  $f_{\max, \text{windon}}$ , it is not represented in the figure.

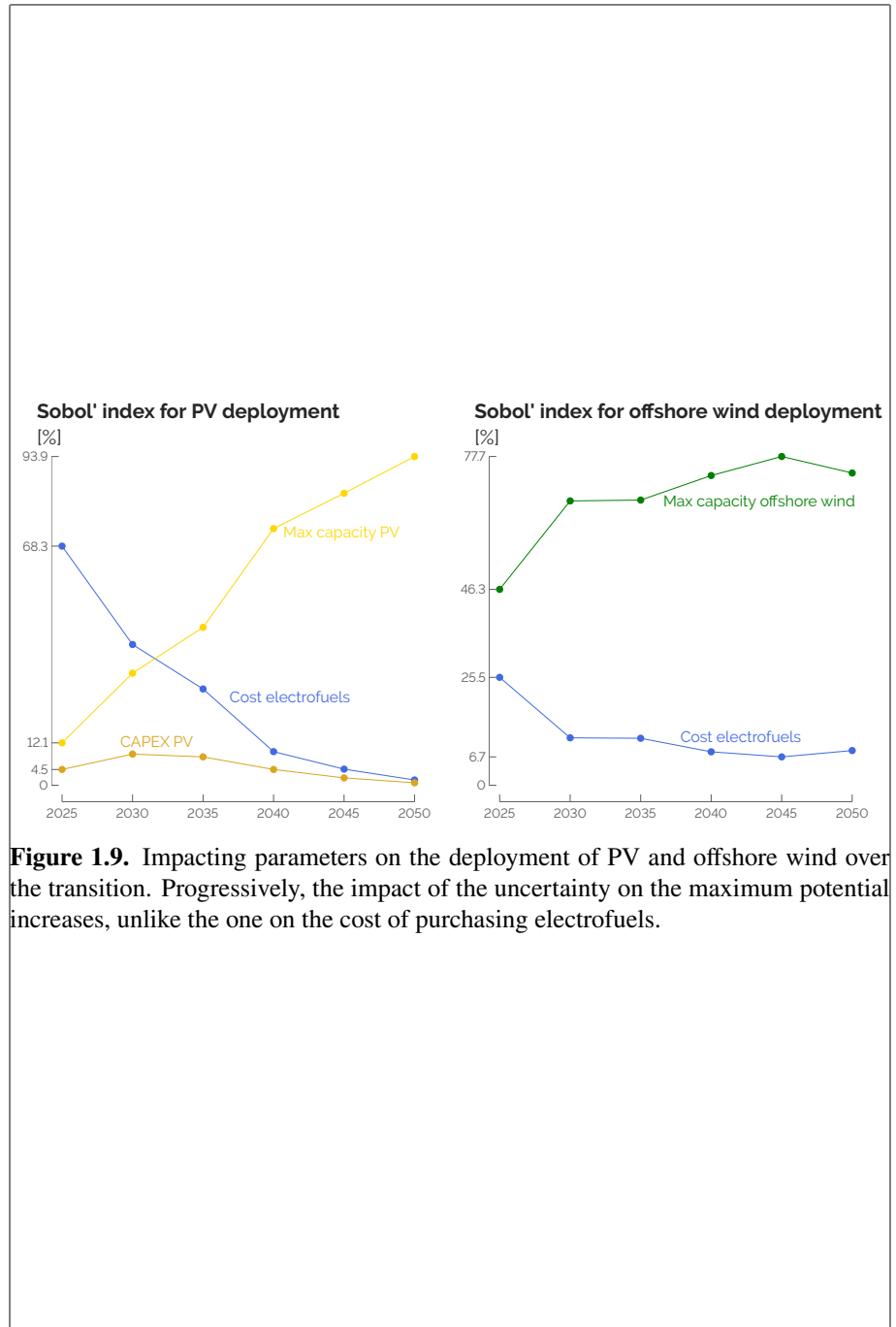
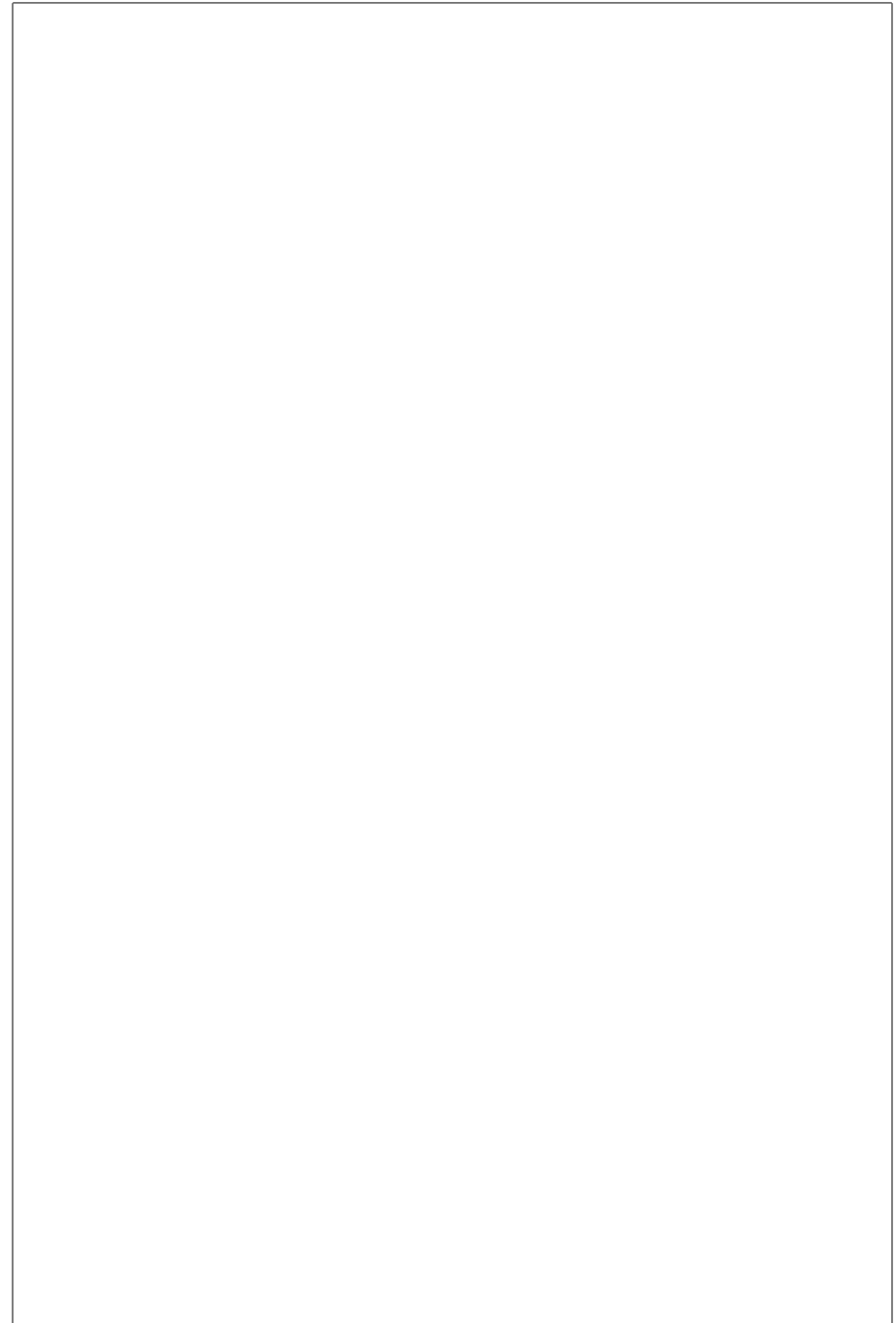


**Figure 1.9.** Impacting parameters on the deployment of PV and offshore wind over the transition. Progressively, the impact of the uncertainty on the maximum potential increases, unlike the one on the cost of purchasing electrofuels.

---

---



---

---

---

## Bibliography

- [1] Climact, VITO, New scenarios for a climate neutral Belgium by 2050, Technical Report, 2021. URL: <https://klimaat.be/doc/climate-neutral-belgium-by-2050-report.pdf>.
- [2] C. F. Heuberger, I. Staffell, N. Shah, N. Mac Dowell, Impact of myopic decision-making and disruptive events in power systems planning, *Nature Energy* 3 (2018) 634–640.
- [3] IEA, Nuclear power and secure energy transitions, 2022. URL: <https://www.iea.org/reports/nuclear-power-and-secure-energy-transitions>, license: CC BY 4.0.
- [4] EnergyVille, PATHS2050 - The Power of Perspective, <https://perspective2050.energyville.be/>, 2022 (accessed December 2022).
- [5] B. Padoan, Nucléaire du futur : la Belgique va coopérer avec la Roumanie et l'Italie sur le développement de SMR, *Le Soir* (2023, 8th of November).
- [6] IAEA, Competitiveness of Nuclear Energy: IAEA's Perspective and Study Results for Europe, <https://sdgs.un.org/goals>, February 2018 (accessed February 16, 2024).
- [7] European Commission, REPowerEU Plan, Technical Report, European Commission, 2022.
- [8] G. Limpens, H. Jeanmart, F. Maréchal, Belgian energy transition: What are the options?, *Energies* 13 (2020) 261.
- [9] G. Limpens, EnergyScope Pathway documentation, Accessed 2022. URL: <https://energyscope-pathway.readthedocs.io/en/v1.1/>.

- [10] D. Suna, G. Resch, Is nuclear economical in comparison to renewables?, *Energy Policy* 98 (2016) 199–209.
- [11] H. Khatib, C. Difiglio, Economics of nuclear and renewables, *Energy Policy* 96 (2016) 740–750.
- [12] X. Rixhon, G. Limpens, F. Contino, H. Jeanmart, Taxonomy of the fuels in a whole-energy system, *Frontiers in Energy Research - Sustainable Energy Systems and Policies* (2021). doi:10.3389/fenrg.2021.660073.
- [13] Eurostat, Share of energy from renewable sources, [https://ec.europa.eu/eurostat/databrowser/view/NRG\\_IND\\_REN\\_\\_custom\\_4442440/default/table?lang=en](https://ec.europa.eu/eurostat/databrowser/view/NRG_IND_REN__custom_4442440/default/table?lang=en), (Accessed April 2023).
- [14] G. Limpens, X. Rixhon, F. Contino, H. Jeanmart, Energyscope pathway: an open-source model to optimise the energy transition pathways of a regional whole-energy system, Elsevier in *Applied Energy* 358 (2024). doi:<https://doi.org/10.1016/j.apenergy.2023.122501>.
- [15] P. Turati, N. Pedroni, E. Zio, Simulation-based exploration of high-dimensional system models for identifying unexpected events, *Reliability Engineering and System Safety* 165 (2017) 317–330.
- [16] World Nuclear Association, Economics of nuclear power, August 2022. URL: <https://world-nuclear.org/information-library/economic-aspects/economics-of-nuclear-power.aspx>.
- [17] D. Coppitters, F. Contino, Optimizing upside variability and antifragility in renewable energy system design, *Scientific Reports* 13 (2023) 9138.
- [18] B. Pickering, F. Lombardi, S. Pfenninger, Diversity of options to eliminate fossil fuels and reach carbon neutrality across the entire european energy system, *Joule* 6 (2022) 1253–1276.
- [19] M. M. Dekker, V. Daioglou, R. Pietzcker, R. Rodrigues, H.-S. de Boer, F. Dalla Longa, L. Drouet, J. Emmerling, A. Fattah, T. Fotiou, et al., Identifying energy model fingerprints in mitigation scenarios, *Nature Energy* 8 (2023) 1395–1404.
- [20] B. S. Palmintier, Incorporating operational flexibility into electric generation planning: Impacts and methods for system design and policy analysis, Ph.D. thesis, Massachusetts Institute of Technology, 2013.

- [21] D. Connolly, H. Lund, B. V. Mathiesen, M. Leahy, A review of computer tools for analysing the integration of renewable energy into various energy systems, *Applied Energy* 87 (2010) 1059–1082. doi:10.1016/j.apenergy.2009.09.026.
- [22] M. G. Prina, M. Lionetti, G. Manzolini, W. Sparber, D. Moser, Transition pathways optimization methodology through EnergyPLAN software for long-term energy planning, *Applied Energy* 235 (2019) 356–368. doi:10.1016/j.apenergy.2018.10.099.
- [23] M. G. Prina, G. Manzolini, D. Moser, B. Nastasi, W. Sparber, Classification and challenges of bottom-up energy system models - a review, *Renewable and Sustainable Energy Reviews* 129 (2020) 109917.
- [24] M. Chang, J. Z. Thellufsen, B. Zakeri, B. Pickering, S. Pfenninger, H. Lund, P. A. Østergaard, Trends in tools and approaches for modelling the energy transition, *Applied Energy* 290 (2021) 116731.
- [25] R. Atlason, R. Unnþorsson, Ideal EROI (energy return on investment) deepens the understanding of energy systems, *Energy* 67 (2014) 241–245. doi:10.1016/j.energy.2014.01.096.
- [26] Pfenninger and Pickering, Calliope - a multi-scale energy systems modelling framework, Accessed 2023. URL: <https://www.callio.pe/>.
- [27] A. University, EnergyInteractive.NET, Accessed July 17th, 2018. URL: <http://energyinteractive.net/>.
- [28] Ž. Popović, B. Brbaklić, S. Knežević, A mixed integer linear programming based approach for optimal placement of different types of automation devices in distribution networks, *Electric Power Systems Research* 148 (2017) 136–146.
- [29] Berkeley Lab, Der-cam, Accessed June 12th, 2023. URL: <https://gridintegration.lbl.gov/der-cam>.
- [30] A. Zerrahn, W.-P. Schill, Long-run power storage requirements for high shares of renewables: review and a new model, *Renewable and Sustainable Energy Reviews* 79 (2017) 1518–1534.
- [31] University of Stuttgart, European Electricity Market Model, Accessed June 12th, 2023. URL: [https://www.iєr.uni-stuttgart.de/forschung/modelle/E2M2/](https://www.iер.uni-stuttgart.de/forschung/modelle/E2M2/).

- [32] S. Backe, C. Skar, P. C. del Granado, O. Turgut, A. Tomasdard, Empire: An open-source model based on multi-horizon programming for energy transition analyses, SoftwareX 17 (2022) 100877.
- [33] Quintel Intelligence, Energy transition model, Accessed September 17th, 2023. URL: <https://docs.energytransitionmodel.com/main/intro/>.
- [34] H. Lund, J. Z. Thellufsen, Energyplan - advanced energy systems analysis computer model (version 15.1), <https://doi.org/10.5281/zenodo.4001540>, 2020. [Accessed September 17, 2020].
- [35] O. Lugovoy, V. Potashnikov, energyRt: Energy systems modeling toolbox in R, development version, 2022. URL: <https://github.com/energyRt/energyRt>, r package version 0.01.21.9003.
- [36] G. Limpens, S. Moret, H. Jeanmart, F. Maréchal, Energyscope td: A novel open-source model for regional energy systems, Applied Energy 255 (2019) 113729.
- [37] Fraunhofer ISI, Enertile, Accessed June 12th, 2023. URL: <https://www.enertile.eu/enertile-en>.
- [38] C. F. Heuberger, Electricity systems optimisation with capacity expansion and endogenous technology learning (eso-xel), Zenodo (2017).
- [39] K. Löffler, K. Hainsch, T. Burandt, P.-Y. Oei, C. Kemfert, C. Von Hirschhausen, Designing a model for the global energy system—genesys-mod: an application of the open-source energy modeling system (osemosys), Energies 10 (2017) 1468.
- [40] L. Herc, A. Pfeifer, F. Feijoo, N. Duić, Energy system transitions pathways with the new h2res model: a comparison with existing planning tool, e-Prime-Advances in Electrical Engineering, Electronics and Energy 1 (2021) 100024.
- [41] R. Dufo López, ihoga, Accessed June 12th, 2023. URL: <https://ihoga.unizar.es/en/>.
- [42] P. Kuhn, Iteratives Modell zur Optimierung von Speicherausbau und-betrieb in einem Stromsystem mit zunehmend fluktuierender Erzeugung, Ph.D. thesis, Technische Universität München, 2012.
- [43] Electric Power Research Institute, Open distribution system simulator (opendss), Accessed June 12th, 2023. URL: <https://sourceforge.net/projects/electricdss/>.

- [44] Energy Exemplar, Plexos (version 9.0), 2023. URL: <https://plexos9.com/>.
- [45] V. Waucquez, Validation of the cost optimization model, pathway energyscope, for scenario analysis, 2023. URL: <http://hdl.handle.net/2078.1/thesis:40534>.
- [46] T. Brown, J. Hörsch, D. Schlachtberger, Pypsa: Python for power system analysis, arXiv preprint arXiv:1707.09913 (2017).
- [47] T. Brown, J. Hörsch, D. Schlachtberger, PyPSA: Python for Power System Analysis, 2018. URL: <https://pypsa.org/>.
- [48] T. T. Pedersen, E. K. Gøtske, A. Dvorak, G. B. Andresen, M. Victoria, Long-term implications of reduced gas imports on the decarbonization of the european energy system, Joule 6 (2022) 1566–1580.
- [49] Energistyrelsen, Modelldokumentation – Ramses energisystemmodel , Technical Report, 2023. URL: [https://ens.dk/sites/ens.dk/files/Analyser/ramses\\_energisystemmodel.pdf](https://ens.dk/sites/ens.dk/files/Analyser/ramses_energisystemmodel.pdf).
- [50] W. Short, P. Sullivan, T. Mai, M. Mowers, C. Uriarte, N. Blair, D. Heimiller, A. Martinez, Regional energy deployment system (ReEDS), Technical Report, National Renewable Energy Lab.(NREL), Golden, CO (United States), 2011.
- [51] R. Loulou, U. Remme, A. Kanudia, A. Lehtila, G. Goldstein, Documentation for the times model part ii, Energy technology systems analysis programme (2005).
- [52] IEA-ETSAP, Times model description, 2021. URL: <https://wiki.openmod-initiative.org/wiki/TIMES>.
- [53] G. Haydt, V. Leal, A. Pina, C. A. Silva, The relevance of the energy resource dynamics in the mid/long-term energy planning models, Renewable energy 36 (2011) 3068–3074.
- [54] S. Pfenninger, J. Keirstead, Renewables, nuclear, or fossil fuels? Scenarios for Great Britain’s power system considering costs, emissions and energy security, Applied Energy 152 (2015) 83–93. doi:10.1016/j.apenergy.2015.04.102.
- [55] B. Pickering, R. Choudhary, Quantifying resilience in energy systems with out-of-sample testing, Applied Energy 285 (2021) 116465.

- [56] S. Pfenninger, Dealing with multiple decades of hourly wind and pv time series in energy models: A comparison of methods to reduce time resolution and the planning implications of inter-annual variability, *Applied energy* 197 (2017) 1–13.
- [57] H.-K. Bartholdsen, A. Eidens, K. Löffler, F. Seehaus, F. Wejda, T. Burandt, P.-Y. Oei, C. Kemfert, C. v. Hirschhausen, Pathways for germany’s low-carbon energy transformation towards 2050, *Energies* 12 (2019) 2988.
- [58] M. Welsch, P. Deane, M. Howells, B. Ó. Gallachóir, F. Rogan, M. Bazilian, H.-H. Rogner, Incorporating flexibility requirements into long-term energy system models—a case study on high levels of renewable electricity penetration in ireland, *Applied Energy* 135 (2014) 600–615.
- [59] G. Limpens, Pathway extension of model EnergyScope TD, Accessed 2023. URL: [https://github.com/energyscope/EnergyScope\\_pathway/tree/v1.1](https://github.com/energyscope/EnergyScope_pathway/tree/v1.1).
- [60] V. Codina Gironès, S. Moret, F. Maréchal, D. Favrat, Strategic energy planning for large-scale energy systems: A modelling framework to aid decision-making, *Energy* 90, Part 1 (2015) 173–186. doi:10.1016/j.energy.2015.06.008.
- [61] F. Y. Kuo, I. H. Sloan, Lifting the curse of dimensionality, *Notices of the AMS* 52 (2005) 1320–1328.
- [62] P. Gabrielli, M. Gazzani, E. Martelli, M. Mazzotti, Corrigendum to “Optimal design of multi-energy systems with seasonal storage” [Appl. Energy (2017)], *Applied Energy* 212 (2018) 720. doi:10.1016/j.apenergy.2017.12.070.
- [63] J. Després, S. Mima, A. Kitous, P. Criqui, N. Hadjsaid, I. Noiro, Storage as a flexibility option in power systems with high shares of variable renewable energy sources: a POLES-based analysis, *Energy Economics* 64 (2017) 638–650. doi:10.1016/j.eneco.2016.03.006.
- [64] P. Nahmmacher, E. Schmid, L. Hirth, B. Knopf, Carpe diem: A novel approach to select representative days for long-term power system modeling, *Energy* 112 (2016) 430–442.
- [65] J. E. Gentle, L. Kaufman, P. J. Rousseeuw, Finding Groups in Data: An Introduction to Cluster Analysis., John Wiley & Sons 47 (2006) 788. doi:10.2307/2532178.

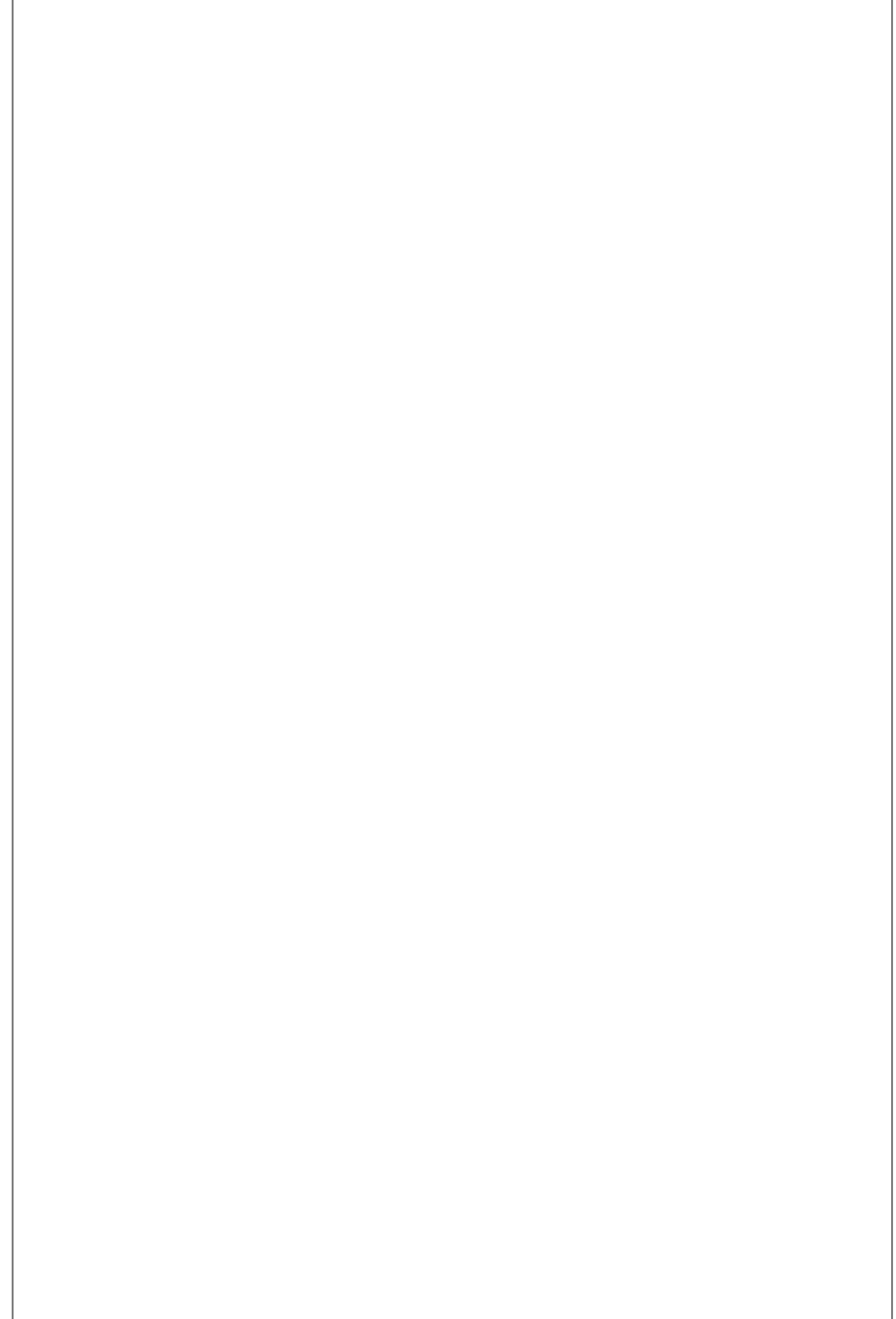
- [66] H. S. Park, C. H. Jun, A simple and fast algorithm for K-medoids clustering, *Expert Systems with Applications* 36 (2009) 3336–3341. doi:10.1016/j.eswa.2008.01.039.
- [67] F. Contino, S. Moret, G. Limpens, H. Jeanmart, Whole-energy system models: The advisors for the energy transition, *Progress in Energy and Combustion Science* 81 (2020) 100872. URL: <https://doi.org/10.1016/j.pecs.2020.100872>.
- [68] X. Rixhon, G. Limpens, D. Coppitters, H. Jeanmart, F. Contino, The role of electrofuels under uncertainties for the belgian energy transition, *Energies* 14 (2021) 4027.
- [69] G. Limpens, S. Moret, G. Guidati, X. Li, F. Maréchal, H. Jeanmart, The role of storage in the Swiss energy transition, in: proceedings of ECOS 2019 conference, 2019, pp. 761–774.
- [70] M. Borasio, S. Moret, Deep decarbonisation of regional energy systems: A novel modelling approach and its application to the italian energy transition, *Renewable and Sustainable Energy Reviews* 153 (2022) 111730.
- [71] J. Dommissé, J.-L. Tychon, Modelling of Low Carbon Energy Systems for 26 European Countries with EnergyScopeTD : Can European Energy Systems Reach Carbon Neutrality Independently?, Master's thesis, UCLouvain, 2020. URL: <http://hdl.handle.net/2078.1/thesis:25202>.
- [72] P. Thiran, H. Jeanmart, F. Contino, Validation of a method to select a priori the number of typical days for energy system optimisation models, *Energies* 16 (2023) 2772.
- [73] M. Pavičević, P. Thiran, G. Limpens, F. Contino, H. Jeanmart, S. Quoilin, Bi-directional soft-linking between a whole energy system model and a power systems model, in: 2022 IEEE PES/IAS PowerAfrica, IEEE, 2022, pp. 1–5.
- [74] J. Schnidrig, R. Cherkaoui, Y. Calisesi, M. Margni, F. Maréchal, On the role of energy infrastructure in the energy transition. case study of an energy independent and co2 neutral energy system for switzerland, *Frontiers in Energy Research* 11 (2023) 1164813. URL: <https://doi.org/10.3389/fenrg.2023.1164813>. doi:10.3389/fenrg.2023.1164813.
- [75] G. Limpens, Generating energy transition pathways: application to Belgium, Ph.D. thesis, Université Catholique de Louvain, 2021.

- [76] G. Limpens, EnergyScope TD documentation, Accessed 2023. URL: <https://energyscope.readthedocs.io/en/v2.2/>.
- [77] IPCC, Climate Change 2013 - The Physical Science Basis, 2014. URL: <https://www.ipcc.ch/report/ar5/wg1/>.
- [78] SPF Economie, Energy - key data - edition february 2022, Brussels, Februrary 2022.
- [79] D. Devogelaer, J. Duerinck, D. Gusbin, Y. Marenne, W. Nijs, M. Orsini, M. Pairon, Towards 100% renewable energy in Belgium by 2050, Technical Report, 2013.
- [80] M. Cornet, J. Duerinck, E. Laes, P. Lodewijks, E. Meynaerts, J. Pestiaux, N. Renders, P. Vermeulen, Scenarios for a Low Carbon Belgium by 2050, Technical Report November, Climact, VITO, 2013.
- [81] Bureau Fédéral du Plan, Perspectives de l'évolution de la demande de transport en belgique à l'horizon 2030, 2015.
- [82] Société Française d'énergie nucléaire, La belgique repousse de 10 ans sa sortie du nucléaire, <https://www.sfen.org/rgn/la-belgique-repousse-de-10-ans-sa-sortie-du-nucleaire/>, January 2023 (accessed April 17, 2023).
- [83] D. Devogelaer, Fuel for the future - More molecules or deep electrification of Belgium's energy system by 2050, Technical Report, Federal Planning Bureau, 2013.
- [84] A. Dubois, J. Dumas, P. Thiran, G. Limpens, D. Ernst, Multi-objective near-optimal necessary conditions for multi-sectoral planning, arXiv preprint arXiv:2302.12654 (2023).
- [85] IEA, Net Zero by 2050, Technical Report, IEA, 2021. URL: <https://www.iea.org/reports/net-zero-by-2050>.
- [86] IRENA, World Energy Transitions Outlook: 1.5°C Pathway, Technical Report, Internation Renewable Energy Agency, 2021. URL: <https://www.irena.org/publications/2021/Jun/World-Energy-Transitions-Outlook>.
- [87] A. Widuto, Energy transition in the EU, Technical Report, European Parliamentary Research Service, 2023. URL: [https://www.europarl.europa.eu/RegData/etudes/BRIE/2023/754623/EPRS\\_BRI\(2023\)754623\\_EN.pdf](https://www.europarl.europa.eu/RegData/etudes/BRIE/2023/754623/EPRS_BRI(2023)754623_EN.pdf).

- [88] Fédération Belge et Luxembourgeoise de l'automobile et du cycle, Automotive Pocket Guide Belgium - Chiffres clefs, Technical Report, 2021. URL: <https://www.febiac.be/public/statistics.aspx?FID=23>.
- [89] F. F. Nerini, I. Keppo, N. Strachan, Myopic decision making in energy system decarbonisation pathways. a uk case study, *Energy strategy reviews* 17 (2017) 19–26.
- [90] I. Keppo, M. Strubegger, Short term decisions for long term problems—the effect of foresight on model based energy systems analysis, *Energy* 35 (2010) 2033–2042.
- [91] B. Nyqvist, Limited foresight in a linear cost minimisation model of the global energy system, Gothenburg: Master's Thesis in Complex Adaptive Systems, Physical Resource Theory, Chalmers University of Technology (2005).
- [92] F. Hedenus, C. Azar, K. Lindgren, Induced technological change in a limited foresight optimization model, *The Energy Journal* (2006).
- [93] S. Moret, V. Codina Gironès, M. Bierlaire, F. Maréchal, Characterization of input uncertainties in strategic energy planning models, *Applied Energy* 202 (2017) 597–617.
- [94] S. Moret, Strategic energy planning under uncertainty, Ph.D. thesis, EPFL, 2017.
- [95] SPF Economie, Vision and strategy hydrogen, October 2022. URL: <https://economie.fgov.be/sites/default/files/Files/Energy/View-strategy-hydrogen.pdf>.

---

---



---

---

---

## Appendix A

# EnergyScope Pathway: Its choice and its formulation

### A.1 EnergyScope Pathway: The right model to choose

*“Only when single-model results are contextualized by the model’s position in the larger ensemble, the reader would be able to have a complete and correct interpretation of the output”* [19]. Energy system models of varying complexity are valuable tools for guiding policymakers and projecting future trends. These models enable the exploration of different energy scenarios and the assessment of their consequences based on the underlying assumptions. Specifically, techno-economic models play a crucial role in identifying technically feasible pathways for the energy transition while considering the associated economic costs. These models can be classified based on two key factors: technical resolution and simulation horizon, as illustrated in Figure A.1.

Increasing the technical resolution of energy system models often comes at the expense of a shorter simulation horizon, and vice versa. For instance, day-ahead grid operation models prioritise accurate grid resolution and capacity reserves in case of foreseeable deviations, but they may not incorporate long-term market trends. Different model classes cater to various needs, with decreasing technical resolution. These include machine-level control, network dispatch, unit commitment, maintenance, power plant expansion, planning for new infrastructure, and scenario analysis. Each class serves a specific purpose, from fine-grained control within a machine to the exploration of multiple assumptions across different scenarios.

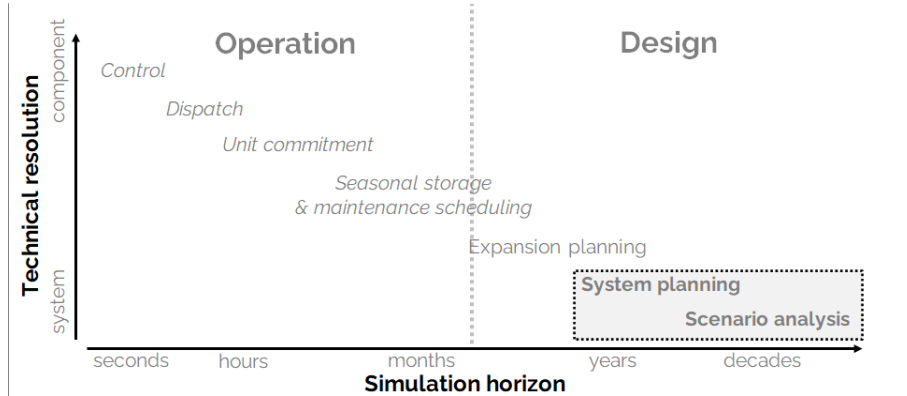


**Figure A.1.** Model can be classified by their core focus: **Operation** or **Design**. These categories can be broken down into subcategories. This paper focuses on the system planning and scenario analysis models. Inspired from [20].

In accordance with the previous classification, models aimed at aiding decision-makers in the energy transition primarily fall under the categories of planning and scenario analysis, with a lower technical resolution than the other classes of model (see Figure A.1). Nonetheless, ensuring technical accuracy is of paramount importance to ensure the effective functionality of future energy systems. Hence, these models should meet the following requirements as a minimum: (i) assessment of intermittent renewable energy integration thanks to an **hourly resolution** spanning a one-year time horizon; (ii) accounting for the **whole-energy system** as including all energy (i.e. heat, electricity, mobility) and non-energy flows in different sectors, accounting for their respective greenhouse gas emissions, as well as all resources, conversion processes, and storage technologies; (iii) exploration of all available options through the **optimisation of investments and operations**; (iv) consideration of long-term investments throughout the **transition pathway** process (i.e. 30 years up to 2050, in our case); and (v) ensuring a reasonable **computational time** (i.e. less than one hour on a personal laptop 15 minutes) for analysing different trajectories. Additionally, to enhance result reproducibility and user understanding, it is advantageous for such models to: (vi) maintain transparency and preferably be **open-source**, with accessible data and accompanied by collaborative documentation.

These requirements are commonly found in reviews of energy system models. In 2010, Connolly et al. [21] reviewed 68 tools, considering similar criteria (i.e. (i-iv) and (vi)), along with others such as the number of users and market equilibrium. In

2019, Prina et al. [22] reviewed 12 “*most established*” models, focusing on criteria (i-ii) and (iv). This review was followed by a classification where criteria (i-iv) were taken into account [23]. In 2021, Chang et al. [24] conducted a survey-based review of 42 models for energy transition modelling, covering all criteria except computational time. Based on these reviews, Table A.1 compares models based on all the previous criteria except the computational time (v). Indeed, the latter is hard to compare as models are not applied to the same case study and the information is rarely given. The table includes only the models that achieved partially at least four out of the five criteria. We endeavored to refresh the model’s information by consulting the model’s website and repository, yet there is a possibility that some information might have been overlooked or omitted inadvertently.

From Table A.1, four models almost check all the boxes (partially the pathway one): Calliope, GENeSYS-MOD, PyPSA and TIMES.

### **TIMES**

The TIMES model, short for The Integrated MARKAL-EFOM System, is a well-established framework renowned for its capacity to generate comprehensive energy models. It encompasses a rich array of features, including support for multi-cell modeling, pathway analysis, full-scale representation of energy systems, and the consideration of market equilibrium dynamics, all of which facilitate thorough scenario exploration. This model has a widespread adoption and has been utilized by worldwide institutions such as the International Energy Agency (IEA) or technical ones such as VITO (Vlaamse Instelling voor Technologisch Onderzoek) research institute in their research endeavors. Notably, TIMES was reported as commercial (i.e. not free to download) in 2010 [21]. A more recent survey conducted in 2020-2021 confirmed that the model was using a commercial interface [24]. Recent developments by the IEA-ET SAP have resulted in a version that is compatible with open-source solver CBC. In various studies conducted in different regions, including Canada, Sweden, the EU, and Denmark, TIMES has been shown to utilize 12 to 32 time-slices annually [23]. It is noteworthy that Haydt et al. [53] conducted a study focusing on the electrical sector, using 12 typical days with an hourly resolution, highlighting the sensitivity of results to time resolution. Regarding data accessibility, while some publications partially present the used dataset, the overall accessibility of TIMES data remains an area of ongoing inquiry [52].

### **Calliope**

**Table A.1.** Comparison of existing models that partially satisfy at least four of the five criteria (in alphabetical order). Legend: ✓ criterion satisfied; √ criterion partially satisfied; ✗ criterion not satisfied. Data from [21–24]

Model	Ref.	Hourly	Whole-energy	Optimis. invest. & operation	Pathway	Open-source
Calliope	[25, 26]	✓	✓	✓	✗ <sup>a</sup>	✓
COMPOSE	[27]	✓	✓	✓	✓	✓ <sup>b</sup>
DER-CAM	[28, 29]	✓	✓ <sup>c,d</sup>	✓	✗ <sup>e</sup>	✓ <sup>f</sup>
DIETER	[30]	✓	✓ <sup>d,g</sup>	✓	✗ <sup>e</sup>	✓
E2M2	[31]	✓	✓ <sup>c,d,h</sup>	✓	✓	✗ <sup>i</sup>
EMPIRE	[32]	✓	✗ <sup>c,d,g,h</sup>	✓	✓	✓ <sup>b</sup>
Ener. Trans. Model	[33]	✓	✓	✗ <sup>j</sup>	✓	✓
EnergyPLAN	[34]	✓	✓	✗ <sup>k</sup>	✗ <sup>l</sup>	✓ <sup>f</sup>
energyRt	[35]	✓	✓	✓ <sup>m</sup>	✓	✓
EnergyScope TD	[36]	✓	✓	✓	✗ <sup>l</sup>	✓
Enertile	[37]	✓	✓ <sup>d</sup>	✓	✓	✗ <sup>n</sup>
ESO-XEL	[38]	✓	✗ <sup>c,d,g,h</sup>	✓	✓	✓
GENeSYS-MOD	[39]	✓	✓	✓	✓	✓
H2RES	[40]	✓	✗ <sup>o</sup>	✓ <sup>??</sup>	✓	✓
iHOGA	[41]	✓	✗ <sup>c,d,g,h</sup>	✓ <sup>m</sup>	✓	✓ <sup>b</sup>
IMAKUS	[42]	✓	✓ <sup>c,d</sup>	✓	✓	✗ <sup>i</sup>
OpenDSS	[43]	✓	✓	✗ <sup>k</sup>	✓	✓
Plexos	[44]	✓	✓ <sup>o</sup>	✓	✓	✗ <sup>i</sup>
PyPSA	[46, 47]	✓	✓	✓	✓ <sup>p</sup>	✓
RamsesR	[49]	✓	✓ <sup>c,d,h</sup>	✓	✓	✓
ReEDS	[50]	✗ <sup>q</sup>	✓ <sup>d,g,h</sup>	✓	✓	✓ <sup>b</sup>
TIMES	[51]	✓	✓	✓	✓	✓ <sup>r</sup>

<sup>a</sup>Topic is being discussed in the chat of their repository but not yet included in their documentation.

<sup>b</sup>‘Free under some special conditions’.

<sup>c</sup> Transport not accounted.

<sup>d</sup> Industry not accounted

<sup>e</sup> Not specified but time horizon is 1 year.

<sup>f</sup> Freeware.

<sup>g</sup> DHN not accounted.

<sup>h</sup> Individual heating not accounted.

<sup>i</sup> Commercially (paid) licensed.

<sup>j</sup>The ETM is a simulation model with a simple merit order ‘optimisation’ for electricity, flex and heat.

<sup>k</sup> Simulation model.

<sup>l</sup> Yearly horizon without pathway.

<sup>m</sup> EnergyRT optimises investments only.

<sup>n</sup> Only for internal use.

<sup>o</sup> Does not account for all sectors but allow to implement them according to Waucquez [45].

<sup>p</sup>Pedersen et al. [48] applied PyPSA to a whole energy system split in 37 nodes. Using a myopic approach, the model optimises the energy transition with a 3-hours resolution).

<sup>q</sup>Seasonal time slice.

<sup>r</sup>Model is now open-source with limited access to data [52].

Calliope is a “*tool that makes it easy to build energy system models*” at different geographical scale. Even if the framework offers the possibility of modelling multi-year systems, we did not find a relevant publication on this topic. In fact, the model is typically employed for scenario analysis. Previous studies have used the model to investigate the phasing out of fossil and nuclear energies in a multi-regional UK power system [54]. More recently, the model has been applied to analyse a scenario of a multi-energy district in Switzerland [55]. Moreover, the model has been used with decades of weather data. However, its application has been limited to assessing the impact of inter-year variability in wind and PV on the results, rather than evaluating a transition pathway [56].

#### **GENeSYS-MOD**

Similarly GENeSYS-MOD presents some limitations. This model is an application of the open-source energy modelling system (OSeMOSYS), itself represented as a model with a poor time discretisation and a heavy computational burden according to [22]. Löffler et al. [39] applied the model to the world by splitting it into 10 regions and most of the energy demand sectors, the time disaggregation being chosen by the user. For their application they used representative years with three days and two time slice per day.

#### **PyPSA**

Among the open-source models with an active community, PyPSA is one of the best-performing, with a large and active community, development at the state of the art, worldwide applications, and usage not only limited to academia. A study conducted by Bartholdsen et al. [57] centered on Germany employed a representation comprising 16 time slices for representative years. This choice was substantiated by the work of Welsch et al. [58], which demonstrated that this level of temporal granularity yields consistent results in comparison to hourly time resolution over a year. However, it is noteworthy that the utilization of a limited number of time slices may simplify the optimization of storage technologies, especially those designed for inter-month energy storage. This simplification can be viewed as a pragmatic approach to reduce the computational burden while over-simplifying the challenge of accurately integrating intermittent renewable energy sources. Furthermore, PyPSA, a modeling framework recognized for its robustness and active user community, has also been employed to investigate scenarios related to myopic transitions [48].

Hence, it is worth noting that while Calliope, OSeMOSYS, PyPSA and TIMES frameworks have the potential to be used for evaluating a transition pathway, we have not come across any publication that explicitly demonstrates their application to such cases with an hourly time resolution over significant time slices. Hence, it appears that none of the models of Table A.1 fully meets all five criteria outlined in the table, topped with the additional consideration of acceptable computational time. This observation is consistent with the findings presented by Prina et al. [22] who identified two approaches for optimising the energy transition pathway based on the six criteria. The first approach involves running a snapshot model multiple times using an algorithm that optimises the transition path and validates the operability of the system. The second approach aims to extend a snapshot model to represent the entire transition pathway. However, they excluded this option due to the lack of models that met the requirements of being fast enough and easily adaptable. Therefore, they developed a new model based on the first methodology, named EPLANoptTP. It uses a multi-objective evolutionary algorithm to optimise the EnergyPLAN model [34]. To manage computational time, the number of decision variables is limited to three: PV, wind turbine and battery capacities. Thus, the model does not investigate all the options (i.e. criteria (iii)).

For the aforementioned reasons, the current work opted for EnergyScope Pathway, an extension of the open-source and documented EnergyScope TD model [36] listed in Table A.1. The latter has an horizon time of one year and does not account for the pathway from an existing energy system to a long-term target. The pathway version extends the time horizon to decades and accounts for the pathway transition from an existing energy system to a long term target. The computational time is kept low (i.e. around a 15 minutes on a personal laptop), mostly due to keeping the linear formulation after extending the snapshot model. Limpens et al. [14] provides more detailed insights into the modeling choices made during methodological development. In the spirit of the EnergyScope project, the code is fully open-source (under the License Apache 2.0, see repo [59]) with a collaborative documentation [9]. Compared to existing models, EnergyScope Pathway introduces a rapid computational optimisation tool for exploring diverse transition pathways within an entire energy system while maintaining high temporal precision to accurately capture the integration of intermittent renewables. To the best of our knowledge, there are potentially frameworks that could be extended to similar capabilities, but their computational time for similar case study have not been found.

## A.2 EnergyScope Pathway and its linear formulation

EnergyScope Pathway is the extension of EnergyScope TD [36] that follows the snapshot approach [60]. The objective of this section is to present the fundamental variables and constraints of the latter based on which the former was developed. There have been formulation choices to be made but they are not discussed in the current manuscript. However, the interested reader is invited to refer to the Appendix B of [14] for further information in this regard.

### A.2.1 The starting point: a scenario analysis model

#### Typical days to break the curse of dimensionality

In the field of bottom-up energy system modelling<sup>1</sup>, one of the biggest challenges is the time resolution [23]. With the rise of VRES, being able to integrate them and capture their interactions with the rest of the energy system requires an hourly time resolution while optimising a whole year (i.e. 8760 hours), if not a whole transition (i.e. several decades). This long-term target combined with a fine time resolution usually leads to the so-called “curse of dimensionality” [61]. As an example, running EnergyScope TD over each of the 8760 hours to optimise a single target year takes more than 19h [36].

To break this curse, EnergyScope TD, like other models [62–64], relies on a subset representative days called typical days (TDs). This more limited number of days, i.e. 12 in the rest of this thesis, cluster the days of the year that have similar time series of demands (i.e. varying electricity and heat demands) and weather data (i.e. sun, onshore and offshore wind). This way, each day of the year is associated to one of these typical days (see Figure A.2).

Finally, to properly capture the inter days dynamics, EnergyScope TD uses the “Coupling typical days” method from Gabrielli et al. [62]. Among others, this allows representing the dynamics and the seasonality of storage capacities. This method as well as the clustering approach selected in our case, i.e. k-medoids [65, 66], extensively detailed and compared to other methods, in the work of Limpens et al. [36].

#### Overview of the snapshot model

<sup>1</sup>As detailed by Prina et al. [23], bottom-up models offer a detailed analysis of components and interconnections within different energy sectors, allowing for a techno-economic comparison of technologies and assessment of alternatives for achieving energy targets and reducing greenhouse gas emissions. On the contrary, top-down modes, mostly used by economists and administrations, integrate a simplified representation of the energy system as interacting with the other macro-economic sectors.

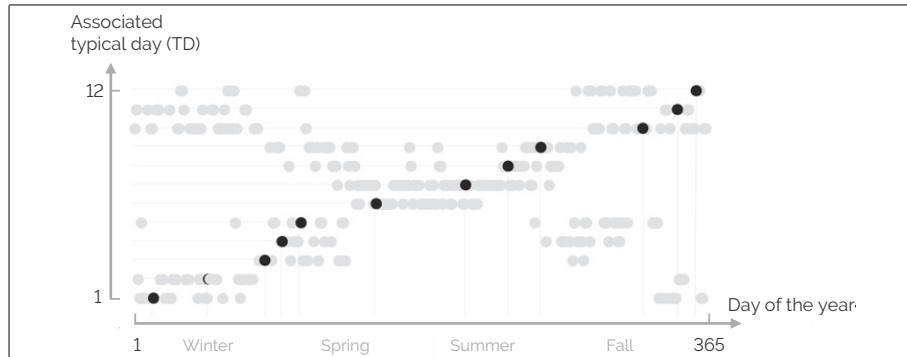


**Figure A.2.** Association of each day of the year (grays) to one of the 12 typical days (TDs) (black dots). Graph adapted from Limpens et al. [36].

EnergyScope TD [36] is a model that optimises both the investment and operating strategy of a '*'whole'*-energy system, encompassing electricity, heating, mobility, and non-energy sectors. According to Contino et al. [67], a model qualifies as a '*'whole-energy'* system when it considers all energy sectors, including the non-energy demand such as the production of plastics and other materials using feedstocks that are also considered as energy carriers, with the same level of detail.

The model's hourly resolution over a year makes it well-suited for integrating intermittent renewables. Its formulation incorporates typical days and a reconstruction method that captures different time scales from the hour to the season while accounting for the inter-weeks patterns of wind. The model investigates all the possibilities by optimising the investment decisions and hourly operations over a year, with a computational time of less than a minute on a personal laptop. This characteristic was intentionally incorporated into the model design to facilitate uncertainty quantification and other studies that require numerous iterations [68].

EnergyScope TD has been successfully applied to various national energy systems, including Switzerland [36, 69], Belgium [8], Italy [70], and other European countries [71]. Furthermore, it has been extended to a multi-region energy system model [72], coupled with other energy models [73], or employed to focus on specific sectors such as the power networks of electricity, gas, and hydrogen [74].

#### Formulation of the snapshot model

The conceptual structure of the model is illustrated in Figure A.3: given the end-use energy demand, the efficiency and cost of energy conversion technologies, the avail-

ability and cost of energy resources, the model identifies the optimal investment and hourly operation strategies to meet the demand and minimise the total annual cost and greenhouse gas emissions of the energy system. Typically, the two objectives are integrated by placing a limit on emissions while simultaneously striving to minimize costs.

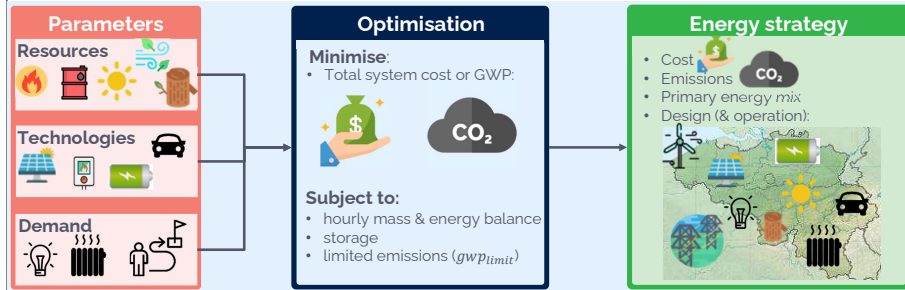


**Figure A.3.** EnergyScope TD model is a flow model with inputs (Parameters), an optimizing model (Optimisation) and results (Energy strategy). The image illustrates what is included (non-exhaustively).

### Linear formulation

The following section illustrates the main constraints of the original EnergyScope TD model. The objective function, cost and GHG formulation will be detailed. The rest of the formulation is detailed and available in previous works [75]. This work uses the following nomenclature: SETs are in capital letters, **Variables** are in bold and with first letter capital, and *parameters* are in italic.

$$\min \mathbf{C}_{\text{tot}} = \sum_{j \in \text{TECH}} \left( \tau(j) \mathbf{C}_{\text{inv}}(j) + \mathbf{C}_{\text{maint}}(j) \right) + \sum_{i \in \text{RES}} \mathbf{C}_{\text{op}}(i) \quad (\text{A.1})$$

$$\text{s.t. } \tau(j) = \frac{i_{\text{rate}}(i_{\text{rate}} + 1)^{\text{lifetime}(j)}}{\left( (i_{\text{rate}} + 1)^{\text{lifetime}(j)} \right) - 1} \quad \forall j \in \text{TECH} \quad (\text{A.2})$$

The objective, Eq. (A.1), is the minimisation of the total annual cost of the energy system ( $\mathbf{C}_{\text{tot}}$ ), defined as the sum of the annualised investment cost of the technologies ( $\tau \cdot \mathbf{C}_{\text{inv}}$ ), the operating and maintenance costs of the technologies ( $\mathbf{C}_{\text{maint}}$ ) and the operating cost of the resources ( $\mathbf{C}_{\text{op}}$ ). The annualised factor  $\tau$  is computed *a priori* based on the interest rate ( $i_{\text{rate}}$ ) and the technology lifetime, ( $\text{lifetime}$ ), Eq. (A.2).

$$\mathbf{C}_{\text{inv}}(j) = c_{\text{inv}}(j) \mathbf{F}(j) \quad \forall j \in \text{TECH} \quad (\text{A.3})$$

$$\mathbf{C}_{\text{maint}}(j) = c_{\text{maint}}(j)\mathbf{F}(j) \quad \forall j \in \text{TECH} \quad (\text{A.4})$$

The total investment cost ( $\mathbf{C}_{\text{inv}}$ ) of each technology results from the multiplication of its specific investment cost ( $c_{\text{inv}}$ ) and its installed capacity ( $\mathbf{F}$ ), see Eq. (A.3). The installed capacity is defined with respect to the main end-uses output type, such as electricity for PV or heat for a boiler. The total operation and maintenance costs ( $\mathbf{C}_{\text{maint}}$ ) are calculated in the same way, Eq. (A.4).

$$\mathbf{C}_{\text{op}}(i) = \sum_{t \in T} c_{\text{op}}(i)\mathbf{F}_t(i, t)t_{\text{op}}(t) \quad \forall i \in \text{RES} \quad (\text{A.5})$$

The total cost of the resources ( $\mathbf{C}_{\text{op}}$ ) is calculated as the sum of the end-use over different periods multiplied by the period duration ( $t_{\text{op}}$ ) and the specific cost of the resources ( $c_{\text{op}}$ ), Eq. (A.5). To simplify the reading, we write the sum over typical days as  $t \in T$  such as in Eq. (A.5) and following equations. The period  $T$  represents the sequence of hours and typical days over a year (8760h)<sup>2</sup>. The full formulation is detailed in [36] or in the documentation [76].

$$\mathbf{GWP}_{\text{tot}} = \sum_{i \in \text{RES}} \mathbf{GWP}_{\text{op}}(i) \quad (\text{A.6})$$

$$\mathbf{GWP}_{\text{op}}(i) = \sum_{t \in T} gwp_{\text{op}}(i)\mathbf{F}_t(i, t)t_{\text{op}}(t) \quad \forall i \in \text{RES} \quad (\text{A.7})$$

The global annual GHG emissions are calculated using a life cycle assessment (LCA) approach, i.e. taking into account emissions of the resources ‘from cradle to use’. It is based on the indicator ‘GWP100a-IPCC2013’ developed by the intergovernmental panel for climate change (IPCC) [77]. For climate change, the natural choice as indicator is the global warming potential, expressed in ktCO<sub>2</sub>-eq./year. In Eq. (A.6), the total yearly emissions of the system ( $\mathbf{GWP}_{\text{tot}}$ ) are defined as the emissions related to resources ( $\mathbf{GWP}_{\text{op}}$ ). The total emissions of the resources are the emissions associated to fuels (from cradle to combustion) and imports of electricity ( $gwp_{\text{op}}$ ) multiplied by the period duration ( $t_{\text{op}}$ ), Eq. (A.7). Thus, this version accounts only for operation without accounting for the GWP emitted during the construction of the technologies. This makes the results comparable with metrics used in the reports by the European Commission and the International Energy Agency (IEA).

The above equations (Eqs. (A.1) - (A.7)) represent only a part of the formulation and illustrate the syntax that is used. Those representing the energy balance, network implementation, sectors representation, etc. are not presented in this work but are detailed in the latest version of the model, see [75] and on the documentation [76].

<sup>2</sup>The exception is storage level which is optimised over the 365 days of the year instead of typical days.

Finally, energy storage has two dimensions to be optimised: the stored energy quantity (also referred to as 'storage level') and the hourly power flow, encompassing both charging and discharging. EnergyScope TD optimises the hourly charge and discharge operations based on the hourly resolution of the typical days. In contrast, the optimisation of stored energy is conducted over the entire span of 8760 hours in a year. This formulation allows for the effective integration of a wide range of energy storage technologies, spanning short-term solutions like small thermal storage units and daily-use batteries, to longer-term options such as hydro-dam storage for seasonal storage, and even large-scale thermal storage for intra-week patterns. A previous study delved into the roles of various storage technologies, considering their sectoral applications and temporal aspects, within the context of the Swiss energy system [69].

### A.2.2 Extending the model for pathway optimisation

In this section, we delve into the extension of EnergyScope TD from a static yearly snapshot model to a comprehensive pathway model. While snapshot models provide insights into the energy system for individual years, they lack the capacity to capture the dynamics inherent in investment strategies throughout a transition period. The proposed approach involves segmenting the transition into five-year intervals. This approach results in seven instances of EnergyScope TD – called representative years – spanning the 30-year transition period, covering the years from 2020 to 2050. To bridge these representative years, we introduce additional constraints that capture the investments changes between consecutive periods, accounting for societal inertia and evaluating both the cost implications and emissions of the transition (see Figure A.4). Overall, these constraints are integrated into a linear framework, ensuring computational efficiency, with an approximate computational time of 14 minutes on a personal laptop (2.4 GHz Intel Core i5 quad-core). Simplification and choices were necessary to implement linearly the problem while keeping a tractable computational time. In this section, we present the formulation retained.

The proposed formulation relies on representative years, selected every 5 years from 2020 to 2050. The period between two of them is called '*PHASE*'. For each of these 7 representative years, the EnergyScope TD model is run using the relevant data (such as energy demand, technology costs or GHG emissions constraints).

As a consequence, a new dimension '*year*' is added to all **Variables** and parameters, except the interest rate ( $i_{rate}$ ) assumed constant during the transition. This new dimension is necessary to represent the changes of technology and resource characteristics over the representative years. As an example, the investment cost ( $c_{inv}$ )

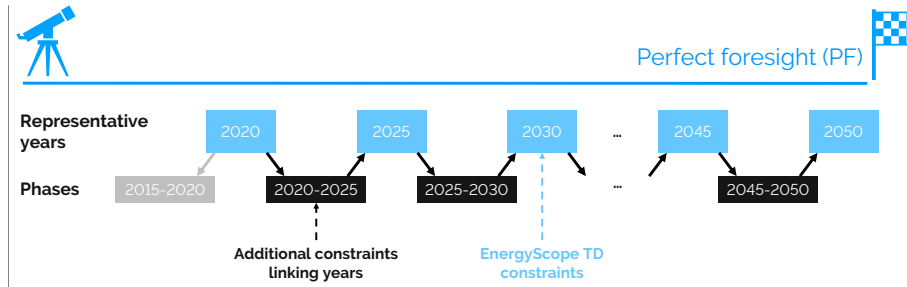


**Figure A.4.** The pathway methodology relies on 7 representative years (blue boxes) where the model EnergyScope Typical Days (EnergyScope TD) is applied. Moreover, the formulation accounts for linking constraints (black boxes) and an initial condition (grey box). The overall problem is the pathway model.

of a solar photovoltaic panels could drastically vary in the next decades (e.g. data used ranges between 1220 to 870 [€<sub>2015</sub>/kW] between 2020 and 2035).

### Linking years

At this stage, all years are independent. In the following, we introduce new constraints to link representative years. The formulation allows to install new capacity ( $\mathbf{F}_{\text{new}}$ ), remove a capacity that has reached its lifespan ( $\mathbf{F}_{\text{old}}$ ) or decommission a technology prematurely ( $\mathbf{F}_{\text{decom}}$ ). These capacity changes occur during a phase, this implies that there is no capacity change during a representative year. Figure A.5 illustrates the concept.

$$\mathbf{F}(y_{\text{stop}}, i) = \mathbf{F}(y_{\text{start}}, i) + \mathbf{F}_{\text{new}}(p, i) - \mathbf{F}_{\text{old}}(p, i) - \sum_{p2 \in \text{PHASE} \cup \{2015\_2020\}} \mathbf{F}_{\text{decom}}(p, p2, i)$$

$$\forall p \in \text{PHASE}, y_{\text{stop}} \in Y\_STOP(p), y_{\text{start}} \in Y\_START(p), i \in \text{TECH} \quad (\text{A.8})$$

Similarly to a mass balance, Eq. (A.8) is the technology capacity balance. The constraint forces the installation or withdrawing of capacities between two representative years: at the end of the phase ( $y_{\text{stop}}$ ), the available capacity is the one used in the next representative year ( $\mathbf{F}(y_{\text{stop}})$ ). This capacity is equal to the one available in the previous representative year ( $\mathbf{F}(y_{\text{start}})$ ) plus the new installed capacity ( $\mathbf{F}_{\text{new}}$ ) minus the capacity that has reached its lifetime ( $\mathbf{F}_{\text{old}}$ ) minus the early decommissioned capacity ( $\mathbf{F}_{\text{decom}}$ ). One notices that the capacity available for each representative year depends on a year ( $y_{\text{start}}$  or  $y_{\text{stop}}$ ), while the other capacity changes depend on a phase ( $p$  or  $p2$ ). Moreover, the decommissioning term depends on another phase, which is the one

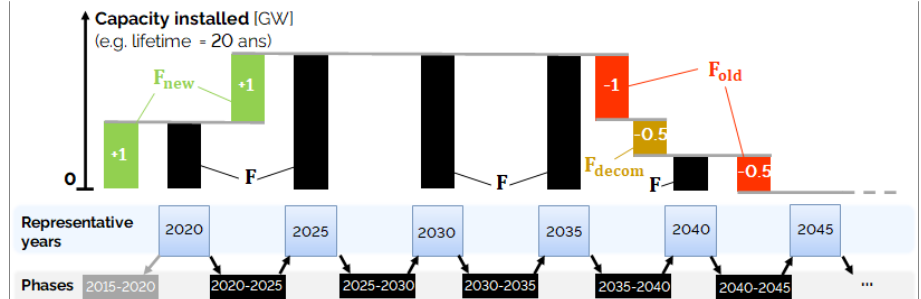


**Figure A.5.** Example of how the technologies capacity and associated variables are evolving. The example uses a technology with a 20 years lifetime. Initially 1 GW of capacity exists ( $F_{\text{new}}$  during phase 2015\_2020). Then another 1 GW is deployed ( $F_{\text{new}}$  during phase 2020\_2025). 15 years later, a part of the capacity reaches its lifetime limit and is removed ( $F_{\text{old}}$  phase 2035\_2040). Moreover, during the latter phase, additional capacity is decommissioned prematurely ( $F_{\text{decom}}$ ). Finally, the technology reaches its expected lifetime and is fully withdrawn ( $F_{\text{old}}$ ).

when the technology decommissioned has been built. As an illustration, Figure A.5 gives an example where 0.5 GW of a capacity built in 2015\_2020 is decommissioned in 2030\_2035 ( $F_{\text{decom}}(2030\_2035, 2015\_2020, i)$ ).

$$F_{\text{decom}}(p, p2, i) = 0$$

$$\forall i \in TECH, p \in PHASE, p2 \in PHASE \cup \{2015\_2020\} | decom_{allowed}(p, p2) = 0 \quad (\text{A.9})$$

$$F_{\text{old}}(p, i) = \begin{cases} \text{if}(age = \text{'STILL\_IN\_USE'}) \text{ then } 0 \\ \text{else } \left( F_{\text{new}}(age, i) - \sum_{p2 \in PHASE} F_{\text{decom}}(p2, age, i) \right) \end{cases}$$

$$\forall p \in PHASE, \forall j \in TECH | age \in AGE(p, j) \quad (\text{A.10})$$

In linear programming, a solution might be mathematically correct, while not making sense in practice. As an example, a technology could be decommissioned before being built ( $p < p_{\text{built}}$ ). Eqs. (A.9-A.10) allow preventing these non-sense while keeping the formulation linear. Eq. (A.9) forces the decommissioned capacity to zero when technology will be built after. To do so, a parameter ( $decom_{allowed}$ ) is defined *a priori* and is equal to 0 or 1 when decommissioning is not possible or possible, respectively. Eq. (A.10) defines the capacity reaching its lifetime limit at a certain phase, the concept is illustrated in Figure A.5. For each phase, a set ( $AGE$ ) is calculated *a priori*. It

relates, for a given phase and technology, when the technology should have been built. In the case the technology has already reached its lifetime limit, the set (*AGE*) returns the phase when the technology has been built. The first part of Eq. (A.10) indicates that the technology is still available, and thus no capacity needs to be removed. The second part of the equation represents the capacity that reached its expected lifetime minus a part of the capacity that would have been decommissioned. As an example, Figure A.5 shows a 20 years lifetime technology with 1 GW of capacity installed before 2020. Ones will highlight the use of a ‘if’ in Eq. (A.10), this formulation is linear as the if is applied to a parameter and not a variable.

$$\mathbf{F}_{\text{new}}(2015\_2020, i) = \mathbf{F}(YEAR\_2020, i) \quad \forall i \in TECH \quad (\text{A.11})$$

To initialise the problem in 2020 with the existing design, an additional phase ‘2015\_2020’ is created. Eq. (A.11) requires that the capacity used in 2020 is installed in the previous phase.

### Society inertia

To avoid unrealistically fast changes in the system, additional constraints are needed during the phases for the mobility and low temperature heat sectors. Without the following constraints, the model would eliminate certain technologies in one phase, such as oil and gas decentralised boilers. Even if this result is mathematically and physically correct, (i.e. fuels are expensive and investing in more efficient technology is economically and environmentally more profitable), this swap of technology cannot occur in one phase (i.e. 5 years). Indeed, society inertia to change, available manpower, supply chains and manufacturers limit the change.

$$\Delta_{\text{change}}(p, i) \geq \sum_{t \in T} (\mathbf{F}_t(y_{start}, i, t)) - \sum_{t \in T} (\mathbf{F}_t(y_{stop}, i, t)) \quad \forall j \in TECH, p \in PHASE, y_{start} \in Y\_START(p), y_{stop} \in Y\_STOP(p) \quad (\text{A.12})$$

$$\sum_{i \in TECH(HeatLowT)} \Delta_{\text{change}}(p, i) \leq lim_{LT,ren} \cdot (eui(y_{start}, HotWater) + eui(y_{start}, SpaceHeat)) \quad \forall p \in PHASE, y_{start} \in Y\_START(p) \quad (\text{A.13})$$

$$\sum_{i \in TECH(MobPass)} \Delta_{\text{change}}(p, i) \leq lim_{MobPass} \cdot eui(y_{start}, MobPass)) \quad \forall p \in PHASE, y_{start} \in Y\_START(p) \quad (\text{A.14})$$

$$\sum_{i \in TECH(MobFreight)} \Delta_{\text{change}}(p, i) \leq lim_{MobFreight} \cdot eui(y_{start}, MobFreight)$$

$$\forall p \in \text{PHASE}, y_{start} \in Y\_START(p) \quad (\text{A.15})$$

Eq. (A.12) calculates the upper limit of change ( $\Delta_{\text{change}}$ ) in terms of supplied demand instead of installed capacity. Based on this quantification, the amount of change per phase is limited for low temperature heat ( $lim_{LT,ren}$ ), Eq. (A.13), passenger mobility ( $lim_{MobPass}$ ), Eq. (A.14) and freight mobility ( $lim_{MobFreight}$ ), Eq. (A.15). For instance, if the maximum allowable variation in supplied low temperature heat is set at 25%, it would restrict the technology-related changes in low temperature heat to 25% within a given phase. Consequently, if a technology supplies more than 25% of the low temperature heat, it would require multiple phases to replace it with a different technology.

### Cost and emissions of the transition

To optimise the energy system, two key metrics must be adapted: the transition cost and the total global warming potential (GWP). Concerning the first one, all costs are expressed in €<sub>2015</sub> and an annualisation factor is used to distinguish investments over the transition. For the GWP, the metric used is based on the contributions of the gases over 100 years. It is assumed that the impact of emitting at the beginning or the end of transition are equivalent and thus no annualisation is used.

$$\min C_{\text{tot,trans}} = C_{\text{tot,capex}} + C_{\text{tot,opex}} \quad (\text{A.16})$$

$$C_{\text{tot,capex}} = \sum_{p \in \text{PHASE} \cup \{2015\_2020\}} C_{\text{inv,phase}}(p) - \sum_{i \in \text{TECH}} C_{\text{inv,return}}(i) \quad (\text{A.17})$$

$$C_{\text{tot,opex}} = C_{\text{opex}}(2020) + t_{\text{phase}} \cdot \tau_{\text{phase}}(p) \cdot \sum_{p \in \text{PHASE} | y_{start} \in P\_START(p), y_{stop} \in P\_STOP(p)} \left( C_{\text{opex}}(y_{start}) + C_{\text{opex}}(y_{stop}) \right) / 2 \quad (\text{A.18})$$

$$\tau_{\text{phase}}(p) = 1 / (1 + i_{\text{rate}})^{\text{diff\_2015\_year}(p)} \quad (\text{A.19})$$

The objective function to be minimised is the total transition cost of the energy system ( $C_{\text{tot,trans}}$ ), defined as the sum of the total capital expenditure (CAPEX) ( $C_{\text{tot,capex}}$ ) and the operational expenditure (OPEX) ( $C_{\text{tot,opex}}$ ), according to Eq. (A.16). The total CAPEX ( $C_{\text{tot,capex}}$ ) is the sum of the investment during each phase ( $C_{\text{inv,phase}}$ ), Eq. (A.17), to which the residual asset investment cost in 2050 is withdrawn ( $C_{\text{inv,return}}$ ). Thus, the investments account for the installation and dismantlement costs of the technologies. The total OPEX ( $C_{\text{tot,opex}}$ ) is the sum of the OPEX in 2020 and the annualised sum of the OPEX during each phase ( $C_{\text{opex}}$ ), Eq. (A.18). During a phase, the system OPEX is the product of the annualised phase factor, defined in Eq. (A.19), and the arithmetic average of OPEX cost for the representative years be-

fore and after the phase. The annualised phase factor is defined based on an average interest rate during the transition.

$$\mathbf{C}_{\text{opex}}(y) = \sum_{i \in \text{TECH}} \mathbf{C}_{\text{maint}}(y, i) + \sum_{j \in \text{RES}} \mathbf{C}_{\text{op}}(y, j) \quad \forall y \in \text{YEARS} \quad (\text{A.20})$$

For each year, the yearly OPEX ( $\mathbf{C}_{\text{opex}}$ ) is the sum of the operating and maintenance costs of technologies ( $\mathbf{C}_{\text{maint}}$ ) and the operating cost of the resources ( $\mathbf{C}_{\text{op}}$ ), Eq. (A.20).

$$\mathbf{C}_{\text{inv,phase}}(p) = \sum_{j \in \text{TECH}} \mathbf{F}_{\text{new}}(p, j) \cdot \tau_{\text{phase}}(p) \cdot (c_{\text{inv}}(y_{\text{start}}, j) + c_{\text{inv}}(y_{\text{stop}}, j)) / 2 \quad \forall p \in \text{PHASE} | y_{\text{start}} \in P\_START(p), y_{\text{stop}} \in P\_STOP(p) \quad (\text{A.21})$$

The investment during a phase ( $\mathbf{C}_{\text{inv,phase}}$ ) results from the multiplication of the newly built technologies ( $\mathbf{F}_{\text{new}}$ ) with their annualised arithmetic averaged specific cost, Eq. (A.21). The annualised phase factor (defined by Eq. (A.19)) is used. The specific cost during the phase is defined as the average between the investment cost for the first and last year of the period.

$$\begin{aligned} \mathbf{C}_{\text{inv,return}}(i) = & \sum_{p \in \text{PHASE} \cup \{2015\_2020\} | y_{\text{start}} \in Y\_START(p), y_{\text{stop}} \in Y\_STOP(p)} \tau_{\text{phase}}(p) \cdot (c_{\text{inv}}(y_{\text{start}}, i) + c_{\text{inv}}(y_{\text{stop}}, i)) / 2 \cdot \\ & \frac{\text{remaining\_years}(i, p)}{\text{lifetime}(y_{\text{start}}, i)} \left( \mathbf{F}_{\text{new}}(p, i) - \sum_{p2 \in \text{PHASE}} \mathbf{F}_{\text{decom}}(p2, p, i) \right) \quad \forall i \in \text{TECH} \end{aligned} \quad (\text{A.22})$$

A part of the investment will remain after 2050. This residual investment, also called salvage value, can be calculated for each technology. A parameter, calculated *a priori*, gives for each technology and construction phase, the remaining amount of years (*remaining\_years*). As an example, if a PV panel has been built in 2045 and has a 20 years lifetime, the parameter will equal to 15 years. Thus, the salvage value is a fraction of the investment cost of this technology when it has been built. This fraction is the ratio between the number of remaining years and the lifetime of the technology. In the previous example, the residual investment of the PV built is 75%. Eq. (A.22) computes, for each technology, the residual value that must be deducted from the total cost. The residual value reflects the fact that the technology can still be used after the horizon of the model and is not fully amortised. The residual value is not applied to technologies that are removed prematurely. This differ from other models, such as Plexos where a technology removed prematurely will benefit from its salvage value (see analysis of [45]).

$$\mathbf{GWP}_{\text{tot,trans}} = \mathbf{GWP}_{\text{tot}}(2020) + t_{\text{phase}} \sum_{p \in \text{PHASE} | y_{\text{start}} \in Y_{\text{START}(p)}, y_{\text{stop}} \in Y_{\text{STOP}(p)}} /2 (\mathbf{GWP}_{\text{tot}}(y_{\text{start}}) + \mathbf{GWP}_{\text{tot}}(y_{\text{stop}})) \quad (\text{A.23})$$

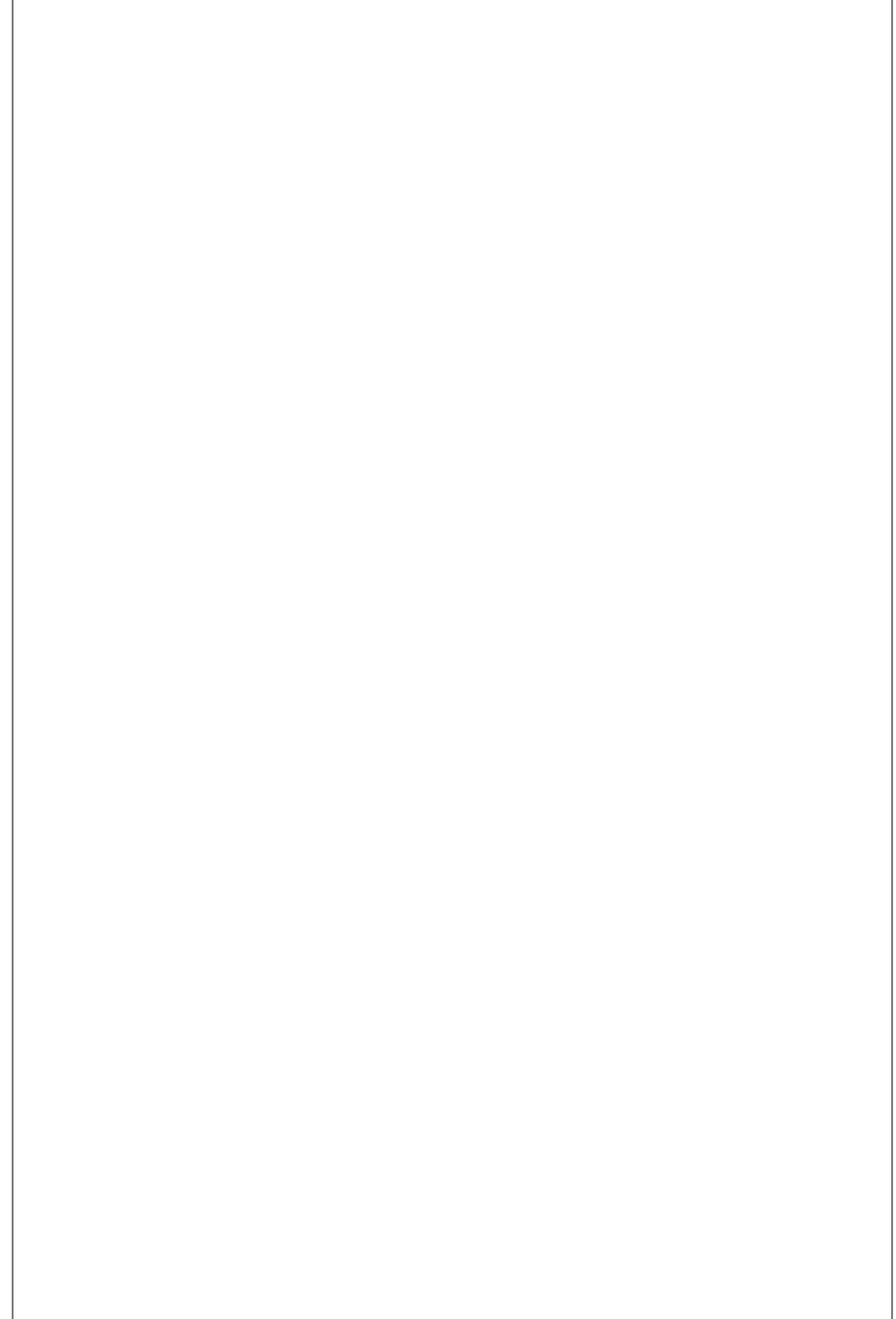
$$\mathbf{GWP}_{\text{tot,trans}} \leq gwp_{\text{lim,trans}} \quad (\text{A.24})$$

The total global warming potential (GWP) emissions during the transition ( $\mathbf{GWP}_{\text{tot,trans}}$ ) are equal to the sum of the total emissions per period ( $\mathbf{GWP}_{\text{tot}}$ ), Eq. (A.23). The emissions during a phase is estimated as the arithmetic average of the representative years before and after the phase. Eq. (A.24) limits the total GWP emissions during the transition by a maximum ( $gwp_{\text{lim,trans}}$ ).

– Appendix 2 - Case study

---

---



---

---

---

## Appendix B

# Case study: the Belgian energy system

### B.1 Belgian energy system in 2020

The Belgian whole-energy system of 2020 was largely based (88.6% of the primary energy mix) on “conventional fuels”(i.e. oil and oil products (38.2%), natural gas (29.5%), uranium (16.3%) and solid fossil fuels (4.6%) while the rest mainly accounts for 26.7 TWh of lignocellulosic and wet biomass, 12.8 TWh of wind and 5.1 TWh of solar [78]. Given the data available in the literature (mostly for the power sector) and, when not available, following the assumptions made by Limpens et al. [8], Table B.1 gives the major technologies used in 2020 to supply the different demands of ??.

### B.2 Belgian energy transition pathway towards carbon-neutrality in 2050

This section presents the results of the deterministic (i.e. all parameters at their respective nominal value) perfect foresight optimisation of the Belgian energy transition pathway constrained to a linear decrease of the GHG emissions from 2020 (121 MtCO<sub>2,eq</sub>) to carbon-neutrality in 2050. After performing a technical investigation of the pathway by checking the greenhouse gas breakdown by energy sectors, the primary energy mix is analysed. To illustrate the sector coupling, a focus is made on the electrification of other sectors. Then, the cost implications in terms of investments and operations are discussed.

**Table B.1.** Major technologies used to supply the 2020-demands of ?? in terms of share of production and installed capacity.

End-use demand	Major technologies	Share of supply	Installed capacity
Electricity	Nuclear	39%	5.9 GW
	CCGT	21%	3.9 GW
	Wind turbines	14%	5.0 GW
Heat High-Temp.	Gas boiler	36%	3.3 GW
	Coal boiler	30%	2.3 GW
	Oil boiler	20%	1.5 GW
Heat Low-Temp. (DEC) <sup>a</sup>	Oil boiler	48%	21.4 GW
	Gas boiler	40%	17.5 GW
	Wood boiler	10%	4.4 GW
Heat Low-Temp. (DHN)	Gas CHP	59%	0.3 GW
	Gas boiler	15%	0.3 GW
	Waste CHP	15%	0.1 GW
Private mobility <sup>b</sup>	Diesel car	49%	93.5 Mpass.-km/h
	Gasoline car	49%	94.7 Mpass.-km/h
	HEV	2%	5.9 Mpass.-km/h
Public mobility	Diesel bus	43%	3.6 Mpass.-km/h
	Train	43%	3.9 Mpass.-km/h
	CNG bus	5%	0.8 Mpass.-km/h
Freight mobility	Diesel truck	74%	62.7 Mt.-km/h
	Diesel boat	15%	10.8 Mt.-km/h
	Train	11%	2.5 Mt.-km/h
HVC	Naphtha/LPG cracking	100%	4.6 GW
Ammonia	Haber-Bosch	100%	1 GW
Methanol	Import	100%	-

<sup>a</sup>The decentralised heating units provide 98% of the low-temperature heat demand.

<sup>b</sup>The private mobility accounts for 80% of the passengers mobility.

### B.2.1 Greenhouse gases and primary energy

Figure B.1 shows the greenhouse gases (GHG) per sector. The system reaches its upper bound (i.e. maximum emissions) every year.

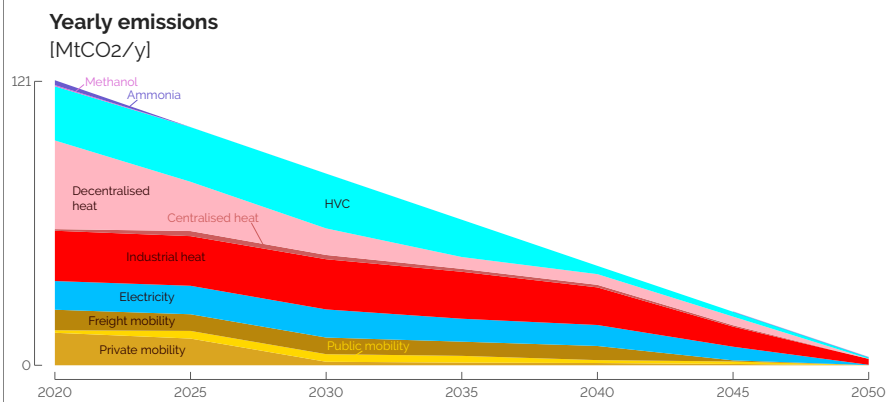


**Figure B.1.** Energy sectors have different speed to reduce GHG emissions over the transition. The system uses all the allowed GHG prescribed by the linear decrease from the emissions in 2020 until carbon-neutrality in 2050.

The defossilisation of the different sectors are not performed at the same rate. The non-energy demand of methanol and ammonia are substituted by electrofuels. These are the first use of electrofuels as e-ammonia is the cheapest electrofuel thanks to the high maturity of the Haber-Bosch process. The decentralised heat and mobility sectors are also dropping first. This is a combination of efficiency and substitution of fossil fuels with electricity. Efficiency comes mainly from district heating networks and electrical heat pumps for the heat sector, and public mobility and electric cars for the mobility sector. From 2040 onward, the decreases are mainly due to the substitution of the remaining fossil fuels by electrofuels as illustrated in Figure B.2.

Figure B.2 shows the primary energy mix for the different representative years. The pathway verifies five trends: (i) reduction of primary energy thanks to energy efficiency; (ii) massive integration of endogenous renewable energies; (iii) importance of electrification; (iv) the usage of gas as the last fossil resource; and (v) the obligation to rely on renewable fuels to achieve carbon neutrality.

The energy supply decreases from 554 TWh/y in 2020 down to 368 TWh/y in 2050 (i.e. -34%) whereas, in the meantime, the demands have increased by 19%, on average. This drop of primary energy consumption reflects the penetration of efficient measures and technologies, such as the previously mentioned public mobility, DHN

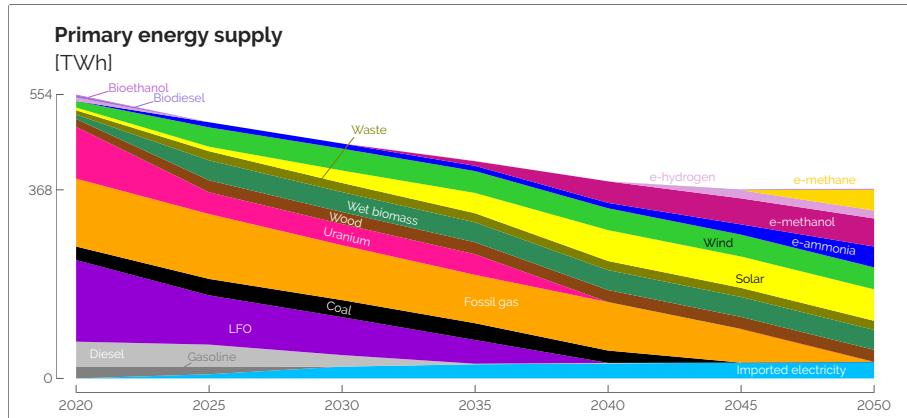


**Figure B.2.** Primary energy emitting GHG (below Uranium) are reducing linearly with fossil gas remaining until 2045. A part of this energy is replaced by renewable ones and starting from 2040, a significant share of electrofuels. As end-use demands slightly increase (see Figure ??), the drop represents energy efficiency (i.e. providing the same services with less primary energy).

or heat pumps. The results in 2050 are aligned with other studies, such as Devogelaer et al. [79]<sup>1</sup> and My2050<sup>2</sup> [1] which estimates respectively a range of 305-417 TWh/y and 307-364 TWh/y for their central scenarios.

The first fossil energy to phase out is gasoline, which is exclusively used for private cars. Indeed, private mobility is partially replaced by public one<sup>3</sup>; and the cars are switching from gasoline and diesel to electricity. Then, diesel and LFO are decreasing. As diesel is used for trucks and buses mobility, it is harder to phase out compared to gasoline exclusively burned in cars. The first drop of LFO reflects the switch from oil boilers to other technologies: heat pumps and gas cogeneration mainly. Then, it is mainly used for the production of HVC, this reflects that HVC is a feedstock hard to defossilise. Finally, coal is kept mainly for industrial usage because it is a cheap fossil fuel (mainly for industrial usage). To phase it out beforehand, a penalty mechanism, such as a carbon tax, would be required, or its strict ban should be put in place. The last

<sup>1</sup>This study was ordered by the National Planning Bureau in 2013. Five scenarios are proposed.

<sup>2</sup>The Climate Change Service of the Federal Public Service Health launched an initiative in 2012 entitled ‘Low Carbon Belgium by 2050’. This initiative resulted in a report and a calculator in 2013 [80]. The Belgian calculator has been improved since then into a recent expert version called **My2050** [1]. From this study, the results of two scenarios will be used: one based on an optimistic evolution of technologies (Technology), and one focusing on an increased dependence on neighbouring countries (EU integration).

<sup>3</sup>Given the major role played by private cars in the Belgian passenger mobility nowadays (i.e. around 80% [81]), public transport (e.g. tramways, buses and trains) is assumed to be able to supply only half of it.

fossil energy present in the system is fossil gas, used for the production of electricity and heat, through cogeneration mainly. Indeed, gas plays a key role to balance the intermittency of solar and wind.

The consumption of uranium declines in 2025, dropping to 2 GW, primarily due to the political framework aimed at phasing out nuclear energy [82]. In the initial stages, significant deployment of endogenous energies takes place. This includes the utilization of wood, wet biomass, and wind energy, followed by the introduction of solar energy. However, solar energy is not fully deployed during this period due to higher integration costs. Starting from 2025, the importation of electrofuels begins, although their significant utilisation is observed from 2035 onwards. Initially, these fuels are predominantly employed as feedstocks in non-energy sectors. From 2040, e-methanol is additionally utilised for the production of High-Value Chemicals (HVCs), e-hydrogen is employed for mobility purposes, and both e-methane and e-ammonia are used for electricity generation through gas CHP and ammonia-based CCGT plants (see Figure B.3).

In 2020, Belgium has been a net-exporter of electricity, however with the shutdown of nuclear power plants and the increase of electricity consumption, Belgium will become a net importer of electricity. These imports reach their maximal allowed capacity by 2035 (i.e. 30% of electricity end use). This strong dependence on imported electricity illustrates the need for balancing intermittent renewables without relying on fossil fuels.

### B.2.2 Electricity sector: Capacities and yearly balance

To better understand the electricity sector, the installed production capacities are given in Figure B.3, while the supply-demand yearly balance is illustrated in Figure B.4.

As introduced in the primary energy analysis (see Figure B.2), renewable capacities soar. By 2050, wind and solar technologies deployments are 60 GW of PV, 10 GW of onshore wind turbines and 6 GW of offshore wind turbines. To compensate the intermittency, the system relies on imported electricity, gas CCGT, sector coupling and storage. This is in line with the work of Devogelaer [83] that ends up with about 80 GW of total installed power generation capacity by 2050, with less PV (i.e. 39 GW) and more wind capacities (i.e. 25 GW of which offshore takes 8.3 GW). As an illustration, in 2050, 176.8 TWh of electricity transit on the grid which includes 32.4 TWh of electricity imported and 15.4 TWh of electricity from CCGT. This result is aligned with other studies that estimates different ranges: 180-310 TWh/y [79], about 250 TWh/y [83], 126-140 TWh/y [1] and in a more recent study using the TIMES-BE model,

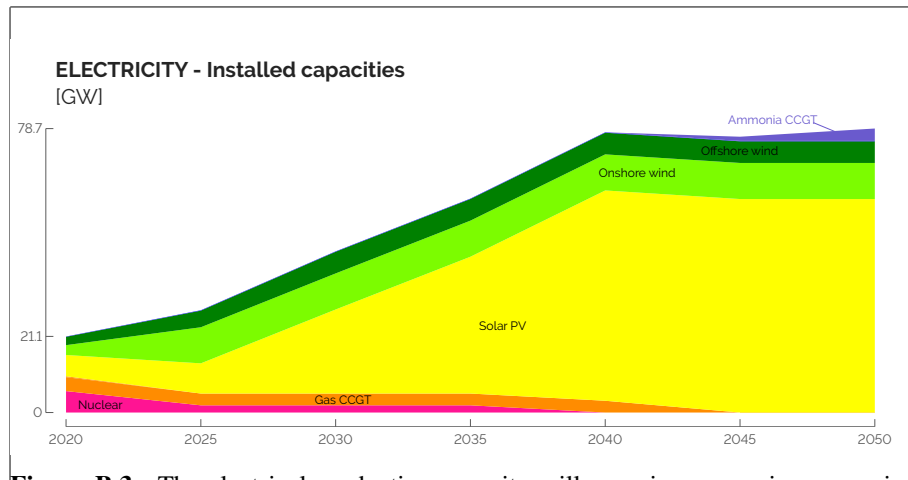


**Figure B.3.** The electrical production capacity will experience massive expansion of wind turbines (onshore and then offshore) and a soaring installed capacity of PV. Ammonia CCGT are installed at the end of the transition to provide a flexible capacity as gas CCGT are phased out.

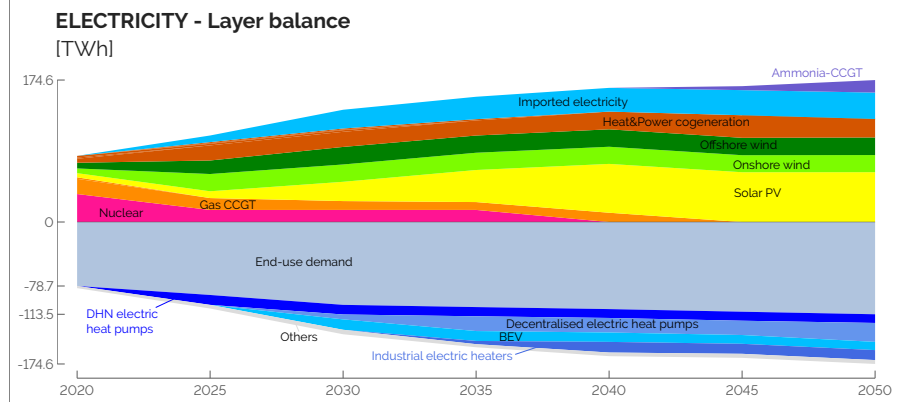


**Figure B.4.** The electricity supply (positive values) will remain a mix of different technologies where backup is first mainly provided by gas-CCGT and then imported electricity, heat and power cogeneration and later ammonia-CCGT. The electricity demand (negative values) is led by the electricity end-use demand, but the share used to electrify heat (heat pumps), vehicles (cars, trains, trams, ...) and industrial heaters drastically increase. This enables a flexible demand that can facilitate the integration of intermittent renewables.

185-196 TWh/y [4]. Higher values from Devogelaer et al. [79] illustrate an almost exclusively electrified energy system. The differences between the study ranges reflect the different assumptions in terms of renewable potentials and availability of nuclear energy. A general trend is that Belgium should maximise its use of endogenous renewable resources, which Dubois et al. [84] identified as a cheaper option than importing additional renewable energies from abroad. Demand management reflects the flexible use of electricity, mainly through heat pumps that uncouple the heat demand and the electricity consumption when combined with thermal storage. Gas CCGT is also a useful asset to compensate intermittent renewables. However, its capacity remains the same as the one installed in 2020. These results are verifying an hourly adequacy of the power demand. Moreover, in a previous study by Pavičević et al. [73], the snapshot version of the model has been coupled with Dispa-SET, a dispatch optimisation model. Results showed that the backup capacity was underestimated by less than 20% to respect reserve capacity, mainly due the lack of reserve capacity for grid stability.

From 2025, the electricity mix has a strong renewable share that rises up to 60% in 2050. The remaining 40% are mainly gas (or ammonia) in CCGT and cogeneration and imported electricity. From a demand perspective, the electrification first starts with DHN heat pumps, then electric cars, then decentralised heat pumps and finally industrial heaters. The latter reflects the usage of cheap PV production peaks.

### B.2.3 Costs: Investments and operation

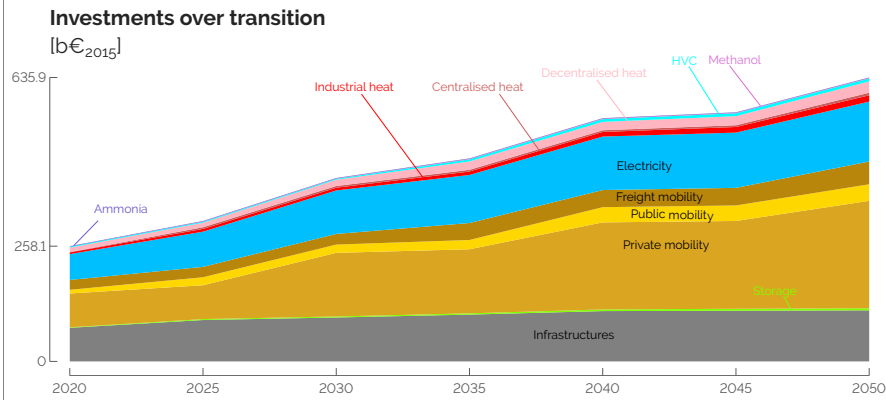
In the following paragraphs, the results are analysed from an economic perspective to decipher the choices made by the model, as the overall cost of the transition is 1 004 b€<sub>2015</sub> split unequally among the sectors.

Figure B.5 illustrates the cumulative investments made throughout the transition, amounting to a total of 377.8 b€<sub>2015</sub>. This makes 12.6 b€<sub>2015</sub> on average per year, which represents 2.1% of the current Belgian gross domestic product (GDP). This is in the range of other studies on climate-neutral scenarios concluding additional investment needs of the order of 2 to 3% of the GDP on a global scale [85, 86] or 2.7 to 3.8% at the European level [87].

Initially, the infrastructure, transport, and electricity sectors each account for approximately one-third of the investments. The investments in infrastructure are primarily driven by the electricity grid and the district heating network (DHN), representing a combined investment of 73 b€<sub>2015</sub>. The electricity sector's investment is led by power plants, totalling 31.5 b€. Notably, the investment costs in the mobility sector are primarily attributed to private cars, constituting 71% of the total. A rough estimation

confirms the significant investment in cars, with an average of 500,000 vehicles registered annually in Belgium over the last decade [88] and assuming an average cost of 20 k€ per car, the funds allocated to private cars amount to 10 b€ per year. This trend in private cars explains why the private mobility sector accounts for half of the investments required to achieve the transition by 2050. This finding aligns with other studies, such as Devogelaer et al. [79], which estimates cumulative investment expenditures of approximately 600 b€<sub>2005</sub> for the transport sector between 2013 and 2050, which confirms our conservative approach in the estimation.

As a comparison, the investments required to fully deploy the PV and wind potentials from 2020 to 2050 amount to 74.4 b€<sub>2015</sub>, with an additional 22.2 b€<sub>2015</sub> allocated to reinforce the grid. The electrification of the heating sectors necessitates investments of 29.2 b€<sub>2015</sub>, including 6.5 b€<sub>2015</sub> for the deployment of the DHN infrastructure. Storage investments, primarily focused on DHN seasonal storage, amount to 3.6 b€<sub>2015</sub>. Apart from the investment required to replace all private vehicles (accounting for 44% of the overall investments), the remaining sectors represent a total of 212 b€<sub>2015</sub>. To mitigate the cost of the transition, My2050 suggests deploying a fleet of no more than one million vehicles and implementing a car sharing system, distinct from car-pooling, as an inevitable measure [1].



**Figure B.5.** The cumulative investments over the transition is unequally spread between the sectors. The energy system in 2020 is imposed to the existing energy system and its expenses are split in three main categories: mobility (mainly vehicles), infrastructure (mainly grids) and electricity (mainly thermal power plants). The investments required during the transition represents 150% the initial investment and mainly in the same three sectors.

A part of the investment will be recovered at the end of the transition based on the remaining lifespan of the technology after 2050. Figure B.6 illustrates the salvage value by sectors, calculated according to Eq. (??). Out of the 114.4 b€<sub>2015</sub> of investments in the infrastructure (i.e. mostly power grid and gas network), 55.9% remain available after 2050, due to their long lifetime. On the contrary, private mobility has a lower salvage value due to a major drop within the first four years and an average lifetime below 10 years [88].

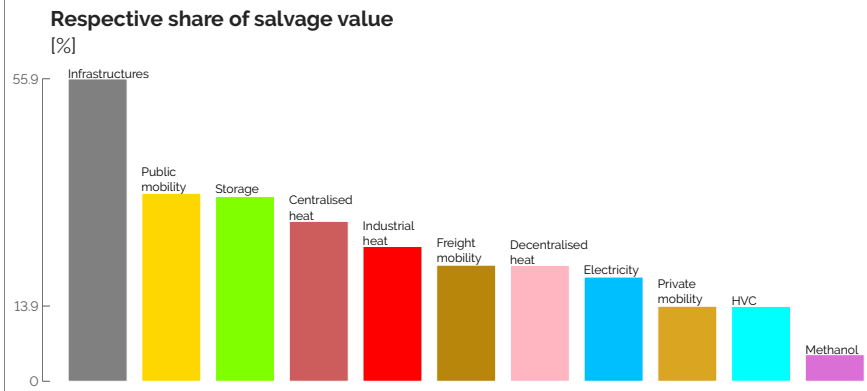


**Figure B.6.** By the end of the transition (i.e. in 2050), the ratio between the salvage value and its cumulative investment, per sector, is unequal. Investments in infrastructures, public mobility, storage and other long-lifetime technologies experience an important salvage value, at the contrary, investments in private mobility will not be recovered as vehicles have a short lifetime. All together, these salvage values represent 160.1 b€<sub>2015</sub>, 25% of the cumulative investment costs in 2050.

In addition to investment decisions, the operational expenditure (OPEX), which accounts for resource utilisation and technology maintenance, are significant. Figure B.7 shows the yearly system cost for each sector except the OPEX related to resources that are grouped together. The latter dominates the OPEX, with a significant share of non-renewable resources (i.e. 63.6% in 2020) until 2040, followed by a steep increase in the share of renewable resources (i.e. 66.2% in 2050). The substantial reliance on non-renewable resources reflects the prevalent use of fossil fuels in our current energy system. The high cost-share of non-renewable fuels underscores the economic challenges of simply substituting fossil fuels with renewables, particularly evident when emphasizing that electrofuels are 2-3 times more expensive. Maintenance expenses in the private mobility sector rank second in terms of expenditure. On the other hand,

maintenance expenses in other sectors are relatively small compared to the aforementioned sectors.

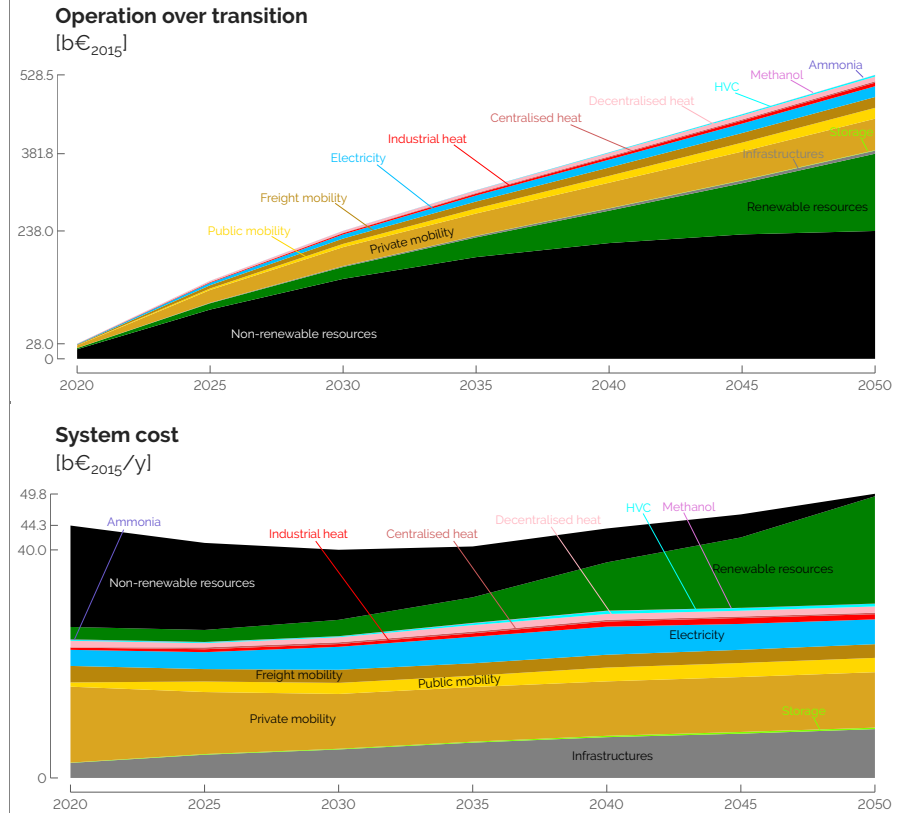


**Figure B.7.** The yearly system cost shows the shift from non-renewable to renewable resources (mainly electrofuels). Operation cost and maintenance represents almost 50% of the expenses.

The annualised cost of the energy system in 2020 is estimated to 44.3 b€/y and increases by 5.5 b€/y to reach 49.8 b€/y by 2050. The work of Climact and VITO [1] estimates the annualised cost in 2050 between 63 and 82 b€/y, while the other studies just indicate the cost increase compared to 2015 (+11.7 to +21) [4, 79]. The differences come from the scope of the energy system: as an example Climact and VITO [1] also account for the agriculture sector. These differences highlight the difficulty to compare different studies due to difference of scope and partial availability of used

data. Overall, comparing with existing studies shows the consistency of the results provided by EnergyScope Pathway.

### B.3 Myopic versus perfect foresight pathway optimisation

This section aims at digging more into the details of the differences observed between the myopic approaches and the reference case (i.e. hourly perfect foresight model).

**Table B.2.** Exhaustive general comparison between the two different foresight approaches: Perfect foresight (PF) and Myopic (MY). Differences with the reference case (PF) below 1% are not shown ( $\simeq$ ) and ones above 10% are in bold.

		PF	MY	Units
Computational time <sup>a</sup>		830	<b>373</b>	s
Costs in 2050	Total transition <sup>b</sup>	1004	$\simeq$	b€ <sub>2015</sub>
	Cumulative opex	528	$\simeq$	b€ <sub>2015</sub>
	Cumulative capex	636	$\simeq$	b€ <sub>2015</sub>
	Salvage value	160	-1%	b€ <sub>2015</sub>
Primary energy mix in 2050	Total	368.0	$\simeq$	TWh/y
	e-hydrogen	15.6	$\simeq$	TWh/y
	e-methane	41.0	+6%	TWh/y
	e-methanol	54.8	$\simeq$	TWh/y
	e-ammonia	40.7	-10%	TWh/y
Electrification in 2050 <sup>c</sup>	System <sup>d</sup>	63.3	$\simeq$	TWh <sub>e</sub>
	Industrial heat <sup>e</sup>	12.3	-7%	TWh <sub>th</sub>
	Decentralised heat <sup>e</sup>	73.9	$\simeq$	TWh <sub>th</sub>
Year of full VRES-deployment	PV	2045	<b>2040</b>	-
	Wind-offshore	2030	<b>2025</b>	-
	Wind-onshore	2025	2025	-

<sup>a</sup>These computational times were reached on a 2.4GHz 4-core machine.

<sup>b</sup>As detailed in ??, the transition cost is the sum of the cumulative opex and capex, salvage value being deduced.

<sup>c</sup>The electrification of the other sectors (i.e. centralised heat (100%-heat pump), private (100%-BEV), public mobility (80%-train and tramway), freight mobility (25%-train) and non-energy demand (0%)) are identical between the three approaches and are, therefore, not presented in the table.

<sup>d</sup>The electrification of the system is computed as the difference between the total production of electricity and the end-use demand of electricity.

<sup>e</sup>The electrification of the industrial and decentralised heating sectors are expressed in terms of thermal energy (TWh<sub>th</sub>) provided by electrified processes, respectively industrial resistors and decentralised electric heat pumps.

Similarly to Nerini et al. [89], Figure B.8 shows that myopic optimisation ends up with a slightly more expensive energy transition by 2050 (i.e.  $+3.2 \text{ b}\epsilon_{2015}$ ), compared to the perfect foresight, despite the savings done at the early stages. Even though this over-cost is negligible compared to the overall cost of the transition (i.e.  $\sim 1000 \text{ b}\epsilon_{2015}$ ), this is explained by the early investments in renewable technologies (i.e. PVs and wind turbines) boosted by the significant salvage value retrieved from investing in the consequent reinforcement of the grid.

Figure B.9 highlights this as infrastructures and the electricity-technologies account respectively for 83.2 and 61.2  $\text{b}\epsilon_{2015}$  in 2030 whereas the overall cumulative investments, so far, are 421.3  $\text{b}\epsilon_{2015}$ . The significant lifetime (e.g. 80 years) and investment cost (i.e. 368M€/GW<sub>VRES</sub> [9]) of the power grid, and, on a smaller scale, the district heating network, explain why the myopic optimisation opts for a higher investment in these infrastructures, at early stages. Similarly to what Keppo and Strubegger [90] observed in their studies, these early investments consequently lead to more investments, later in the transition, to renew technologies that have become too old before 2050: during the phase between 2045 and 2050, the myopic approach needs to invest in 9.2GW of PVs that have been installed 25 years before whereas the perfect foresight, by smoothing its investments over the entire transition, has to renew only 2.5GW of PVs.

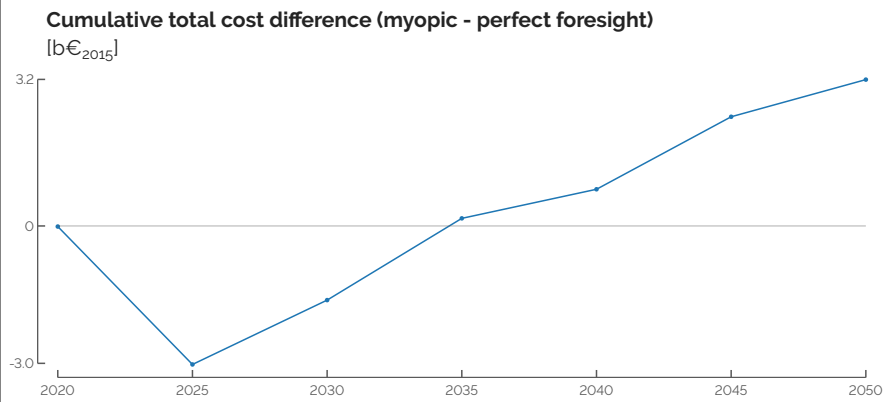


**Figure B.8.** Cumulative total cost (i.e. opex+capex-salvage value) difference between the myopic and perfect foresight (PF) approaches. Positive values mean that the myopic approach is higher than perfect foresight. Early savings of the myopic vision are overcompensated by late investments further on.

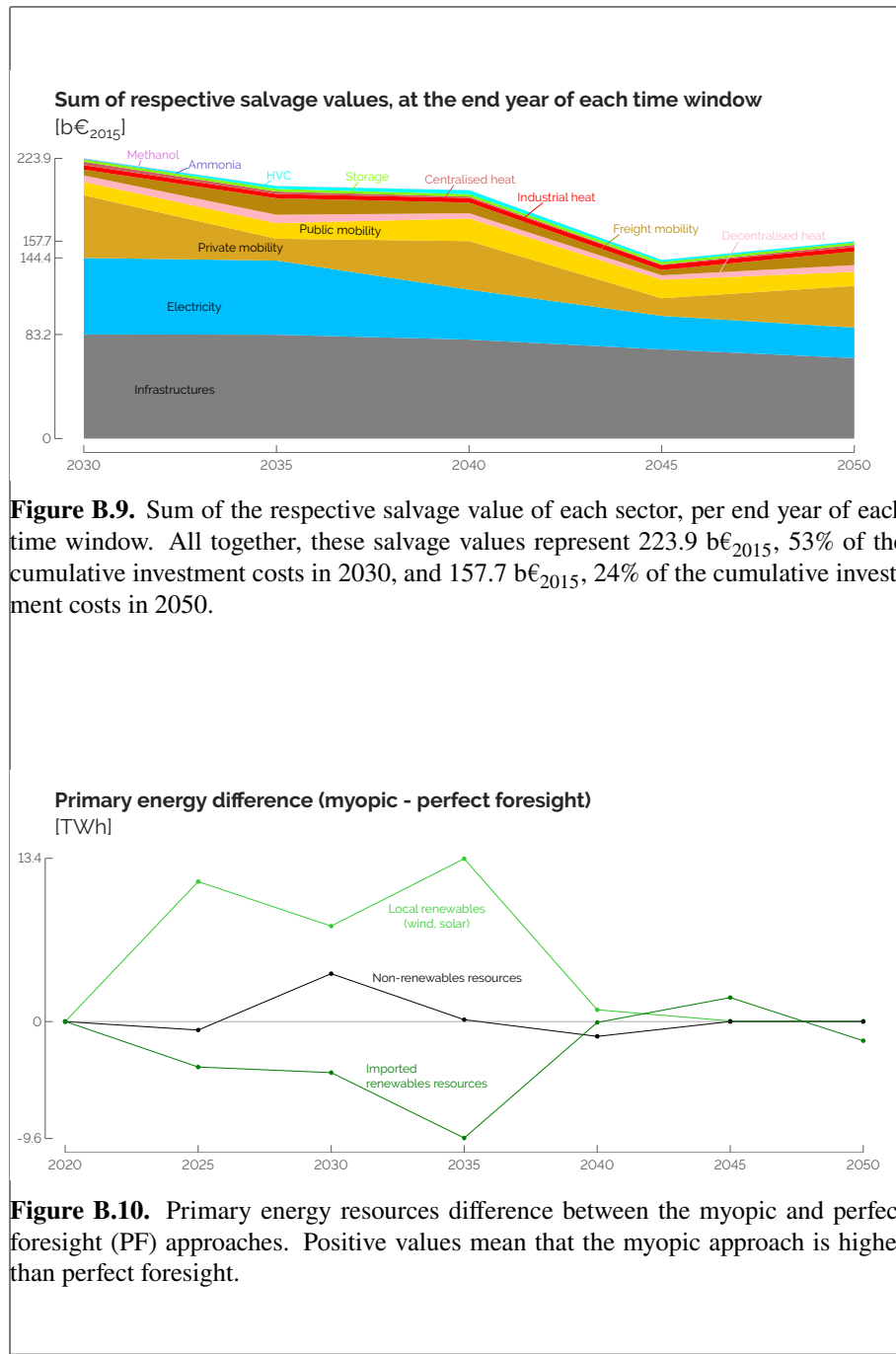
In 2050, the capacities installed in the different sectors, the design of the system in other words, are very similar between the two approaches. The passenger and freight mobility sectors are the same where differences smaller than 1GW are observed in other sectors. More interestingly, the myopic optimisation tends to postpone the decommissioning of capacities when the loss of salvage values at the end of an optimisation window would be bigger than the maintenance cost. For instance, in the myopic approach, 0.8GW of industrial coal boilers will remain installed in 2045 and 2050 or 3.6GW of naphtha-crackers to produce HVC in 2040, whereas these technologies are not used. This is comparable to the "lock-ins" detailed in other studies [2, 90] where technologies installed at early stages of the transition remain in place.

Highlighted in Figure B.10, the earlier availability of renewable (and intermittent) electricity consequently accelerates the electrification of the other sectors. For instance, in 2035, 3.7GW (+75%) more of industrial electric heaters to produce 5.1TWh/year (+130%) of additional industrial heat. In the low-temperature heat sector, decentralised and centralised electric heat pumps capacities are, respectively, 2.2GW (+19%) and 1GW (+8%) higher for each of the representative years between 2030 and 2045, to produce, around 7.8TWh/year (+23%) and 0.8TWh/year (+1%), at the expense of other technologies such as gas heat pumps. Finally, public trains substitute from 2035 a higher share of the CNG-buses.

In general, due to the formulation of the salvage value (see Eq. ??), the myopic approach is more techno-oriented as investing more in technologies is beneficial, especially at the early stages of the transition. Therefore, before converging to a similar energy mix in 2050, the myopic system relies more on local renewables (e.g. solar and wind) than on importing renewable energy carriers (e.g. e-ammonia, e-methanol, e-hydrogen or e-methane), see Figure B.10. In parallel, in the near term, the system relies on average more on conventional/non-renewable sources, like observed in other studies [90–92].

## B.4 Assessment of different emissions-trajectories

This section compare results of the optimisation subject to different emissions-trajectories with the REF case where the emissions are constrained to decrease linearly from the level in 2020 to carbon-neutrality in 2050. The first comparison is done with the trajectory subject to respect the CO<sub>2</sub>-budget prescribed in the reinforcement learning (RL)-based pathway optimisation, i.e. 1.2 Gt<sub>CO<sub>2</sub>,eq</sub> (Section ??). Then, to assess the impact of the myopic approach on the optimisation of the transition, it is compared to perfect foresight results, alleviating the constraint on the emissions-trajectory.



### B.4.1 CO<sub>2</sub>-budget versus linear decrease of emissions

Figure B.11 shows the yearly emissions attributed for each sector in the REF case (i.e. imposed CO<sub>2</sub>-budget) and a case where the CO<sub>2</sub>-trajectory is constrained instead. Interestingly, these two transition pathways end up in a similar carbon-neutral whole-energy system in 2050. The two main sectors that significantly reduce their emissions in the REF case are the production of HVC and the high-temperature heat. In the former, this is linked to the extended use of oil products through naphtha-cracking. The latter is produced by industrial coal boilers for longer, until 2040. Overall, ending up to the same level of emissions in 2050, the REF case represents a 60% reduction of the cumulative emissions compared to the linear decrease, for a 7.5% more expensive transition.

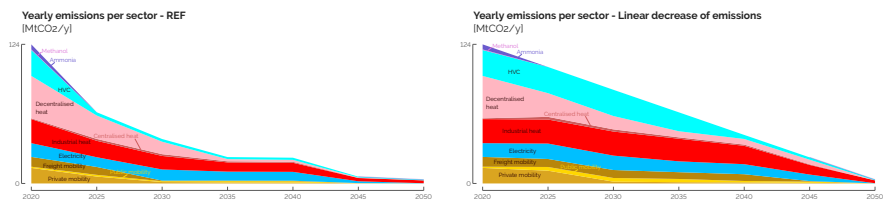


**Figure B.11.** Respecting the CO<sub>2</sub>-budget imposed in the REF case drastically cuts the emissions of the system, especially in the production of high value chemicals (HVC) and the high-temperature heating sector.

### B.4.2 Comparison without restriction on GHG

The outcomes of a model could be limited when the case study is too restrictive. Indeed, ones could argue that the comparison between myopic, monthly and perfect foresight are very similar as the energy system is strongly constrained in terms of GHG emissions.

In the following, we perform a similar comparison in the transition pathway without restricting the GHG emissions.

#### Reference case

Figure B.12 illustrates the transition taken by Belgium without restriction on the GHG emissions.

Similar trends that for the defossilisation are observed: primary energy mix reduces, renewable energy integration rises and an electro-fuel is imported. However,

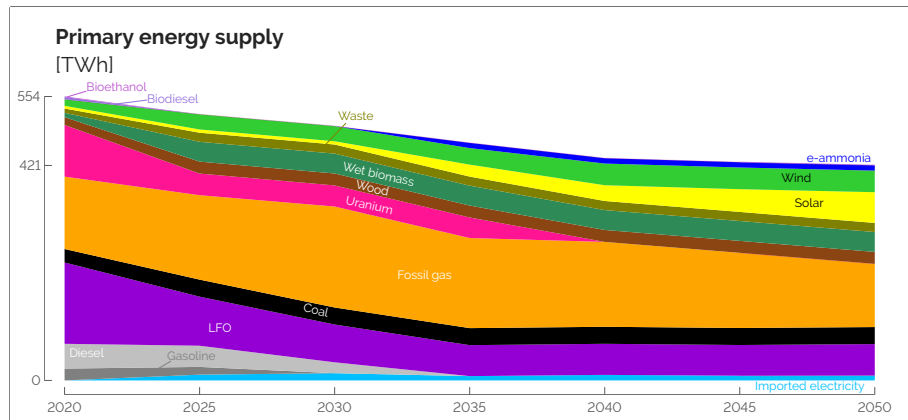


**Figure B.12.** Primary energy mix of a non-constrained energy transition. In this results, carbon neutrality is not reached in 2050. Some fossil fuels remain used.

some changes reflects the cheapest option that the system could utilise to reach a cheaper transition, such as using as little electrofuels as possible. In this case, only e-ammonia is used for its end use demand.

Instead of analysing the energy system in details, the following paragraphs will investigate if the comparison findings are consistent on a different case study.

#### Comparison with Myopic approach

Several key messages of the comparison have been summarised in Table B.2. In the following paragraph we analyse how these conclusions are affected when the constraint on the GHG-emissions trajectory is removed.

First, considering the overall transition cost, the myopic approach keeps on making short-term savings, i.e. down to -0.2%, before ending up with a more expensive transition by 2050, i.e. +0.2%. Similarly to the case with an imposed GHG-emissions trajectory, myopic optimisation invests more, compared to the perfect foresight, at early stages into VRES technologies to benefit from the significant salvage values of the related grid infrastructures. In 2030, the salvage value of the infrastructures and electricity-generation technologies account for 80.2 and 56.2 b€<sub>2015</sub>, respectively, whereas the overall CAPEX are 404.8 b€<sub>2015</sub> by then.

Then, in the case with a prescribed GHG-emissions trajectory, the myopic approach had to invest more by the end of the transition to renew PV installed more massively at early stages and that reached the end of their lifetime before the end of the transition. In the case without this emissions trajectory, there is less an urgency/need for

integrating renewables in the system. Consequently, in the latter case, there is not such an extra-investment to make to renew too old renewable assets. On top of this, the slower uprise of VRES in the case without emissions trajectory leads to a smaller difference of electrification of the other sectors between the perfect foresight and myopic approaches.

Finally, even though the way to get there differs between the perfect foresight and the myopic approaches, the system designs by 2050 are very similar between these two in most of the sectors. The main observed difference is in the freight transport where diesel boats are preferred to gas boats. This can be looked as a result of the lock-in effect where choices made at early stages, due to the limited foresight, remain in place in the longer term.

In essence, when comparing perfect foresight and myopic approaches, distinctions arise in minor aspects, while the fundamental conclusions of Table B.2 were verified. These variances have been elucidated in the preceding enumerated points and can primarily be attributed to the changes in the case study, rather than reflecting limitations inherent to the model or the comparative analysis itself.

## B.5 Uncertainty characterisation for the 5-year steps transition

Table B.3 summarises the uncertainty ranges for the different groups of technologies and resources, for the year 2025. Refer to [93, 94] for the methodology and sources. As the model optimises the system every 5 years,  $N = 5$  has been selected to get the final ranges of uncertainties of type II and III, based on the work of Moret [94]. For type III uncertainties (i.e. uncertainty ranges increasing with time), a 50% increase has been set arbitrarily between the ranges for 2025 and these same ranges for 2050. In other words, for these specific uncertainties, the ranges for 2050 are 50% larger than for 2025.

Rixhon et al. [68] analysed the impact of these parameters on the total cost of the snapshot Belgian whole-energy system in 2050 subject to different GWP limits. Based on this work, we have selected a subset of impacting uncertainties, added others due to the pathway formulation (e.g.  $\Delta_{\text{change,pass}}$ ), and listed them in Table B.3. The uncertainty characterisation gives the uncertainty ranges per parameter or group of parameters (category).

This work considers nine groups of uncertain parameters: (i) the cost of purchasing imported energy carriers; (ii) the investment cost (i.e. CAPEX) of some technologies, mostly related to the mobility sector and the integration of renewables; (iii) the maintenance cost (i.e. OPEX) of every technology; (iv) the consumption of electric and fuel

cells vehicles in the mobility sector; (v) the potential installed capacity of renewables; (vi) the hourly load factor of renewables accounting for variability of solar irradiance or wind speed; (vii) the availability of resources considered as limited (i.e. biomass and electricity); (viii) the end-use-demands split per sector of activities (i.e. households, services, passenger mobility and industry) and (ix) other parameters like the interest rate or the modal share change in different key sectors. For the specific case of SMR, the parameter  $f_{\max,SMR}$  will influence the maximum capacity (i.e. 6 GW) to install to translate somehow the readiness of this technology. If it is (i) smaller than 0.6, there is no possibility to install SMR during the transition; (ii) between 0.6 and 0.8, these 6 GW can be installed only in 2050; (iii) between 0.8 and 0.9, these can be installed from 2045 onward and; (iv) higher than 0.9, the prescribed maximum capacity can be installed from 2040 onward.

**Table B.3.** Application of the uncertainty characterization method to the EnergyScope Pathway model for the year 2025.

Category	Parameter	Meaning	Type <sup>a</sup>	Relative variation <sup>b</sup> min	max
<b>Cost of purchasing</b>	$c_{\text{op,fossil}}$	Purchase fossil fuels	II	-64.3%	179.8%
	$c_{\text{op,elec}}$	Purchase electricity	II	-64.3%	179.8%
	$c_{\text{op,electrofuels}}$	Purchase electrofuels	II	-64.3%	179.8%
	$c_{\text{op,biofuels}}$	Purchase biofuels	II	-64.3%	179.8%
<b>Investment cost</b>	$c_{\text{inv,car}}$	CAPEX car	I	-21.6%	25.0%
	$c_{\text{inv,bus}}$	CAPEX bus	I	-21.6%	25.0%
	$c_{\text{inv,ic\_prop}}$	CAPEX ICE	I	-21.6%	25.0%
	$c_{\text{inv,e\_prop}}$	CAPEX electric motor	I	-39.6%	39.6%
	$c_{\text{inv,fc\_prop}}$	CAPEX fuel cell engine	I	-39.6%	39.6%
	$c_{\text{inv,efficiency}}$	CAPEX efficiency measures	I	-39.3%	39.3%
	$c_{\text{inv,PV}}$	CAPEX PV	I	-39.6%	39.6%
	$c_{\text{inv,grid}}$	CAPEX power grid	I	-39.3%	39.3%
	$c_{\text{inv,grid\_enforce}}$	CAPEX grid reinforcement	I	-39.3%	39.3%
	$c_{\text{inv,nuclear\_SMR}}$	CAPEX SMR <sup>c</sup>	I	-40.0%	44.0%
<b>Maintenance cost</b>	$c_{\text{maint,var}}$	Variable OPEX of technologies	I	-48.2%	35.7%
<b>Consumption</b>	$\eta_{\text{e\_prop}}$	Consumption electric vehicles	I	-28.7%	28.7%
	$\eta_{\text{fc\_prop}}$	Consumption fuel cell vehicles	I	-28.7%	28.7%
<b>Potential installed capacity</b>	$f_{\text{max,PV}}$	Max capacity PV	I	-24.1%	24.1%
	$f_{\text{max,windon}}$	Max capacity onshore wind	I	-24.1%	24.1%
	$f_{\text{max,windoff}}$	Max capacity offshore wind	I	-24.1%	24.1%
<b>Hourly load factor</b>	$c_{\text{p,t,PV}}$	Hourly load factor PV	II	-22.1%	22.1%
	$c_{\text{p,t,winds}}$	Hourly load factor wind turbines	II	-22.1%	22.1%
<b>Resource availability</b>	$avail_{\text{elec}}$	Available electricity import	I	-32.1%	32.1%
	$avail_{\text{biomass}}$	Available local biomass	I	-32.1%	32.1%
<b>End-use demand</b>	$HH\_EUD$	Households EUD	III	-13.8%	11.2%
	$services\_EUD$	Services EUD	III	-14.3%	11%
	$pass\_EUD$	Passenger mobility EUD	III	-7.5%	7.5%
	$industry\_EUD$	Industry EUD	III	-20.5%	16.0%
<b>Miscellaneous</b>	$i_{\text{rate}}$	Interest rate	I	-46.2%	46.2%
	$\%_{\text{pub,max}}$	Max share of public transport	I	-10%	10%
	$\Delta_{\text{change,freight}}$	Modal share change freight mobility	-	-30%	30%
	$\Delta_{\text{change,pass}}$	Modal share change passenger mobility	-	-30%	30%
	$\Delta_{\text{change,LT\_heat}}$	Modal share change LT-heat	-	-30%	30%
	$f_{\text{max,SMR}}$	Potential capacity SMR	-	0	1

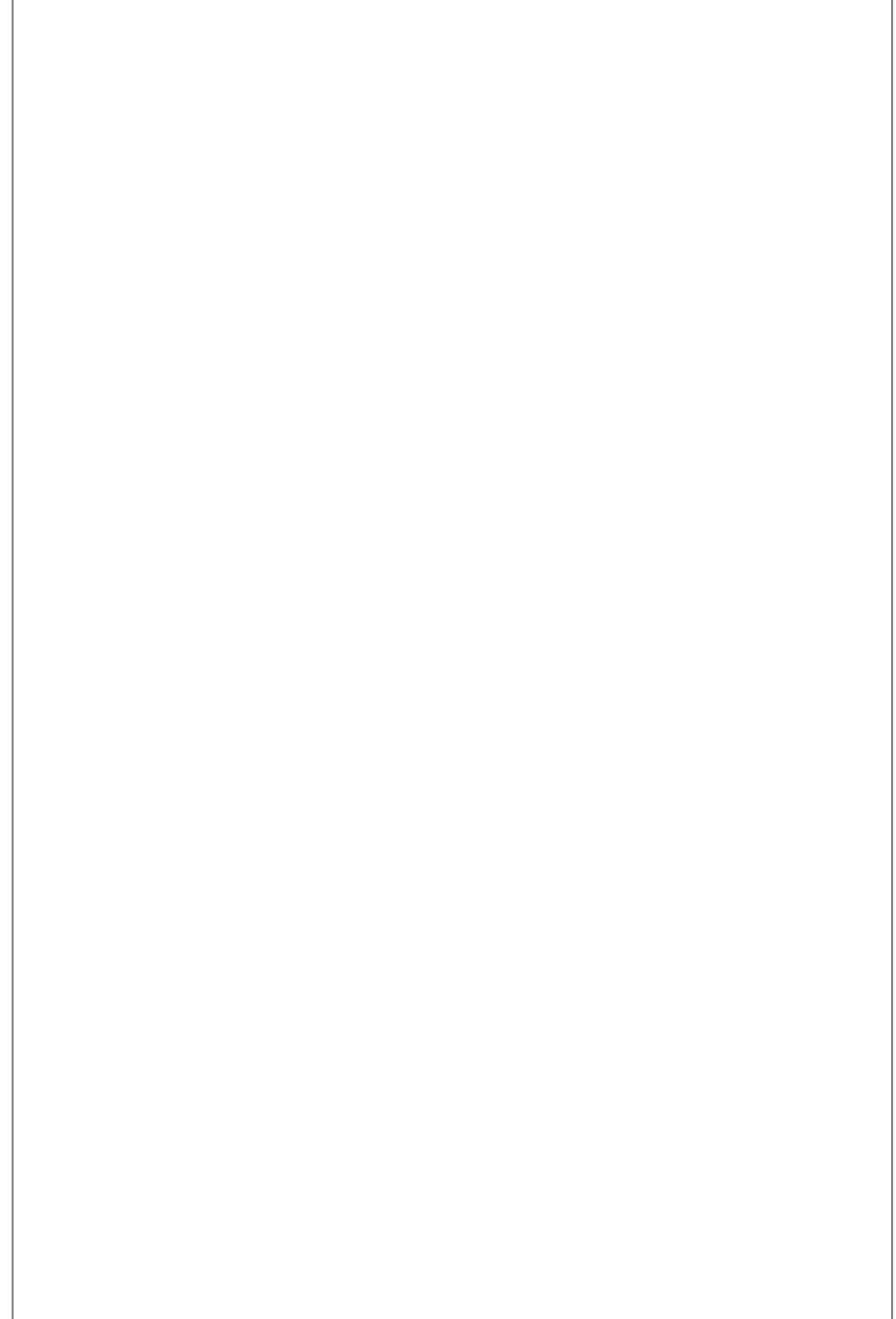
<sup>a</sup>Per Moret [94], “I: investment-type, II: operation-type (constant uncertainty over time), III: operation-type (uncertainty increasing over time)”.

<sup>b</sup>The nominal values of each of the parameters is 0, meaning no variation compared to the nominal values of the impacted parameter in the model.

<sup>c</sup>This range has been inferred from the local sensitivity analysis performed by EnergyVille [4].

---

---



---

---

---

## Appendix C

# Pathway optimisation under uncertainties

### C.1 Total transition cost

Table C.1 gives the ranking and total Sobol index over the total transition cost of each of the 34 parameters listed in Table B.3. The first column shows these indicators for the GSA applied on the monthly pathway model that has some limitations [?] but has the main advantage to run much faster. The second column gives the same indicators but for an uncertainty quantification carried out on the hourly pathway model and only using the most impacting parameters. Given the similar rankings of the parameters between these two, this comparison shows that the monthly model can be a computationally efficient proxy to quantify the uncertainties of the actual hourly model and point out the key parameters on optimisation-driving objective, the total transition cost.

Besides the top-4 parameters, rankings are slightly different. However, this does not jeopardize the comparative analysis given the similar Sobol' indices. Given their wide range of uncertainty [-64.3%; 179.8%] and their significant role to meet the CO<sub>2</sub>-budget, the cost of purchasing electrofuels is the first, by far, impacting parameter. Next, comes, naturally, the industrial EUD, representing, at the nominal value, 60% of the total demands by 2050. The top-3 is completed by the variation of the interest rate, directly impacting the annualisation and the salvage values of the assets. Finally, since the current Belgian whole-energy system deeply relies on fossil resources, and would still do in the near future, the cost of purchasing fossil fuels is part of the impacting parameters. On the contrary, due to the very low annualised, cost, long lifetime leading

to a significant salvage value and a low-emitting fuel, the parameters related to SMR barely impact the total transition cost.

**Table C.1.** Total Sobol' indices of the uncertain parameters over the total transition cost in the monthly and hourly pathway models. The similar rankings (and indices) show the validity of using the faster (even though less accurate) monthly model to assess uncertainties over the hourly model.

<b>Parameter</b>	<b>Ranking (Sobol' index)</b>	
	Monthly model	Hourly model
<b>Purchase electrofuels</b>	1 (47.4%)	1 (44.4%)
Industry EUD	2 (23.5%)	2 (26.4%)
Interest rate	3 (11.0%)	3 (13.2%)
Purchase fossil fuels	4 (6.9%)	4 (6.9%)
Variable OPEX of technologies	5 (2.9%)	6 (3.0%)
Purchase biofuels	6 (2.6%)	5 (3.0%)
Hourly load factor PV	7 (1.9%)	9 (1.3%)
CAPEX electric motor	8 (1.9%)	7 (2.5%)
Hourly load factor wind turbines	9 (1.3%)	8 (1.4%)
Max capacity PV	10 (1.1%)	14 (0.5%)
<b>Potential capacity SMR</b>	11 (0.9%)	11 (1.0%)
Available local biomass	12 (0.8%)	12 (0.7%)
CAPEX car	13 (0.7%)	10 (1.2%)
Passenger mobility EUD	14 (0.7%)	13 (0.7%)
Modal share change LT-heat	15 (0.5%)	-
Households EUD	16 (0.5%)	-
Services EUD	17 (0.4%)	-
Max capacity onshore wind	18 (0.3%)	-
Max share of public transport	19 (0.3%)	-
CAPEX PV	20 (0.2%)	-
Max capacity offshore wind	21 (0.2%)	-
Efficiency electric motor	22 (0.1%)	-
CAPEX fuel cell engine	23 (0.1%)	-
CAPEX ICE	24 (0.1%)	-
Efficiency fuel cell engine	25 (<0.1%)	-
Modal share change freight mobility	26 (<0.1%)	-
Modal share change passenger mobility	27 (<0.1%)	-
CAPEX efficiency measures	28 (<0.1%)	-
CAPEX bus	29 (<0.1%)	-
CAPEX grid reinforcement	30 (<0.1%)	-
CAPEX power grid	31 (<0.1%)	-
<b>CAPEX SMR</b>	32 (<0.1%)	-
Available electricity import	33 (<0.1%)	-
Purchase electricity	34 (<0.1%)	-

## C.2 Imported renewable electrofuels

Figure C.1 gives the distribution of the different routes of supply and consumption of gas like methane, hydrogen, ammonia and methanol, resulting from the 1260 samples of the GSA.

Given its lower cost of purchasing than its renewable equivalent (??) and lower GWP than other fossil fuels (i.e.  $gwp_{op,NG} = 0.27 \text{ kt}_{CO_2,eq}/\text{GWh}$  versus  $gwp_{op,LFO} = 0.31 \text{ kt}_{CO_2,eq}/\text{GWh}$  or  $gwp_{op,coal} = 0.40 \text{ kt}_{CO_2,eq}/\text{GWh}$ ), fossil NG remains the main source of gas in the system until 2040. Besides bio-hydrolysis as the main consumer of wet biomass to consistently produce gas, e-methane eventually substitutes fossil natural gas by 2045-2050 in order to respect the CO<sub>2</sub>-budget for the transition. Its versatility makes gas used by a wide variety of technologies in the different sectors. Initially, in 2020, decentralised gas boilers, CCGT and industrial gas boilers represent the biggest consumers of gas with 39%, 21% and 16% of the total consumption, respectively. Progressively, in line with the rest of the system shifting towards more efficiency in the mid-term, industrial CHP represent the lion's share, next to other usages in the transport or LT-heating sectors.

On the contrary, import of fossil-based hydrogen, largely produced from steam-methane-reforming [95], is rarely part of the solution due to the emissions related to the consumption of natural gas. E-hydrogen is the consistent source of hydrogen in the system, next to local production (i.e. steam-methane-reforming, electrolysis or ammonia-cracking) in some rare cases where low industrial EUD coincides with more abundant electricity from SMR or PV. In terms of consumption, FC-trucks are the more consistent player. FC-cars are also at stake but in specific cases where their CAPEX and the CAPEX of electric vehicles are in the bottom and the top of their respective uncertainty range.

Becoming cheaper than its fossil equivalent at early stages of the transition (i.e. from 2030 onward), e-ammonia is the exclusive stream of ammonia in the system, except rare cases. Then, on top of its consistent NED, the largest consumption of ammonia is CCGT as flexible power generation units, to substitute their e-methane equivalents that have a higher LCOE (??).

Similarly to ammonia, on top of local production in rare cases, e-methanol is the key source for methanol. Besides its own NED, methanol is mostly consumed to produce HVC via the MTO process instead of naphtha-cracking, in order to respect to CO<sub>2</sub>-budget for the transition.

**Table C.2.** Comparison of the quantities of imported renewable electrofuels, in TWh, between the REF case, the SMR case and the statistical features from the GSA (i.e. Q1, median and Q3). 2020 is not in the table as, per assumption, no renewable electrofuel is imported for this year. For the sake of clarity, zeroes are replaced by “-”.

Year	Case	e-methane	e-hydrogen	e-ammonia	e-methanol
2025	REF	-	-	10	52
	SMR	-	-	10	29
	Q1	-	-	9	2
	Median	-	-	10	46
	Q3	-	-	11	55
2030	REF	-	1	10	52
	SMR	-	1	10	52
	Q1	-	-	9	43
	Median	-	-	10	51
	Q3	-	1	12	57
2035	REF	-	17	10	53
	SMR	-	17	10	53
	Q1	-	-	9	44
	Median	-	4	11	52
	Q3	-	16	32	58
2040	REF	-	16	23	54
	SMR	-	16	10	54
	Q1	-	-	12	43
	Median	-	12	36	53
	Q3	10	16	68	60
2045	REF	40	16	42	54
	SMR	-	16	11	54
	Q1	-	-	24	43
	Median	-	13	49	52
	Q3	44	17	77	60
2050	REF	39	16	44	55
	SMR	7	16	11	55
	Q1	-	-	20	44
	Median	19	14	44	53
	Q3	51	17	72	61

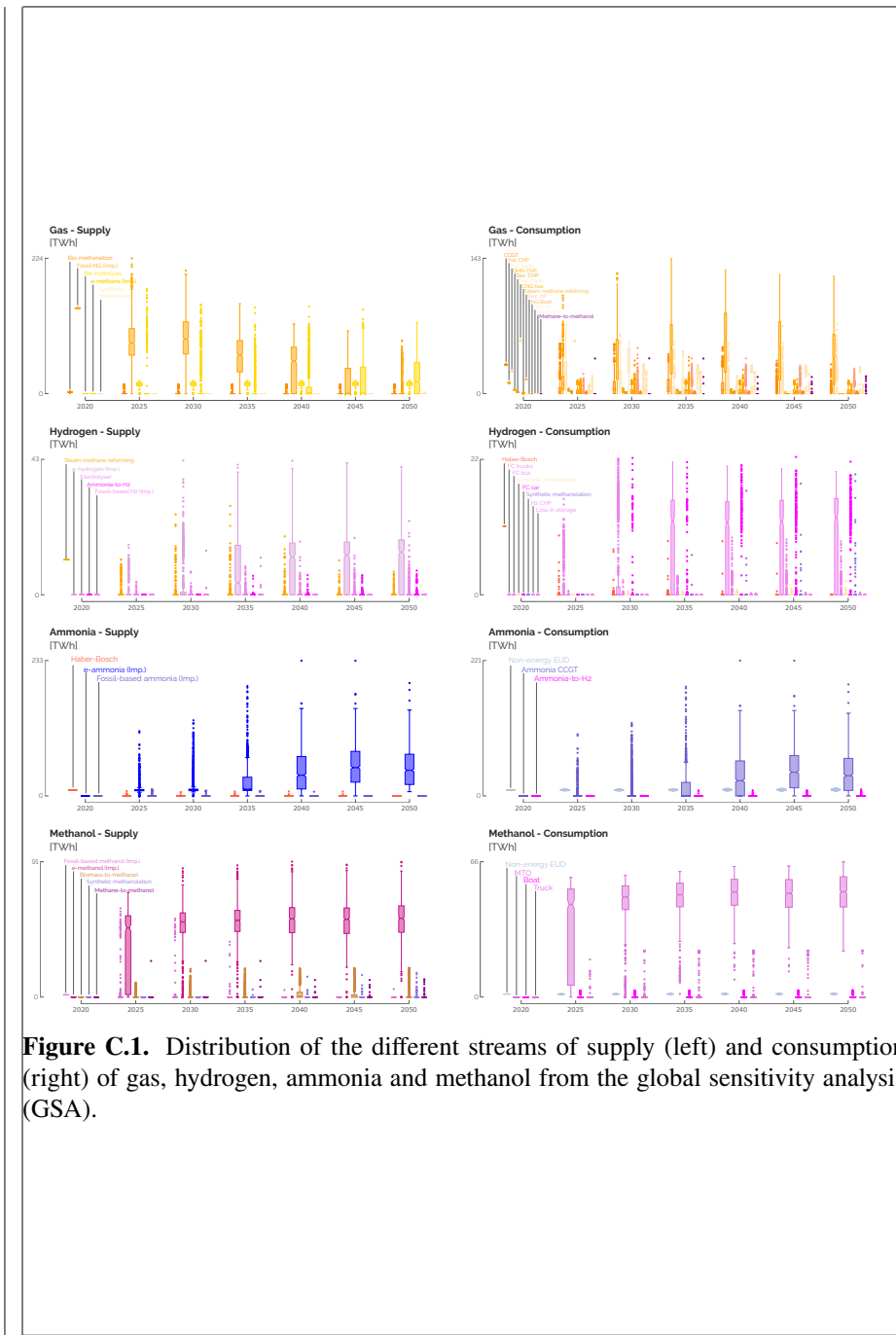


**Figure C.1.** Distribution of the different streams of supply (left) and consumption (right) of gas, hydrogen, ammonia and methanol from the global sensitivity analysis (GSA).